Response to Anonymous Referee #1

Major comments:

1) A new method by considering the variation in MAC is developed to obtain BC mass size distribution and then bulk BC mass concentration from size-resolved light absorption measurements. Size-resolved MAC calculated on the basis of core-shell Mie model is mainly discussed, which is determined by D_p-dependent D_{BC} and coating thickness. However, there are many assumptions in calculation processes, e.g., same DBC and coating thickness at each selected mobility size, a constant number fraction of BC-containing particles, etc. Meanwhile, measurements were not described clearly.

Response: Thanks for your comments. The size resolved MAC in this study was based on core-shell Mie model. The influence of the BC aggregates on the MAC as well as the relative deviation between the core-shell model and BC aggregates were discussed in section 5.1 of the revised manuscript to evaluate the effects of the morphology on MAC. With respect to the assumptions used in this study, their uncertainties were discussed in section 5, such as the uncertainties caused by using idealized core-shell model (section 5.1), by using a constant BC-containing particle fraction (section 5.2) and by variation of refractive index (section 5.3). With respect to description of measurements, a more detailed description of our measurement was added in section 2.

2) The significance of this study should be also strengthened. In my point of view, compared to BC mass loading, the light absorption measurements are more required to evaluate the influences of BC particles on solar radiation. Thus, MAC is likely to be more important for converting bulk BC mass loading, which can be directly measured by using chemical method (e.g., Thermo Optical Reflection-EC) or laser-induced incandescence techniques (e.g., SP2-rBC), to light absorption in climate research. The current study is more important for obtaining BC mass size distribution from size-resolved absorption measurement. BC mass size distribution obtained from the DMA-AE51 measurement based on the new method is also suggested to compare

with that obtained from the direct measurement from DMA-SP2 system, which has used in the field campaign.

Response: Thanks and we agree with your comments. More sentences were added in this text to stress the significance. The main goal of this study was to derive equivalent BC mass concentration (EBC, after Petzold et al. (2013)) more precisely and obtain BC particle mass size distribution (BCPMSD) from size-resolved absorption measurement. MAC is an important variable that has to be discussed in the process. Derivation of the EBC and related uncertainties were more discussed to emphasize that our goal was to determine EBC more precisely.

3) The Mie model is likely to not suitable for the calculation of BC aggregates with large sizes. For a small BC particle (core), the mass equivalent diameter of the assumed BC sphere is much smaller than the wavelength (880 nm) resulting in a less effect of morphology to absorption. In this case, the Mie model is somewhat feasible for absorption estimation. However, for a large BC particle (core), its mass equivalent diameter is close to the wavelength (i.e., large size parameter); thus, the absorption is largely influenced by the morphology. Moreover, large BC particles are more likely to exhibit loose fractal aggregates with thin coating, thus, is likely much different from core-shell structure. MAC in this case cannot be well depicted by using Mie model.

Response: Thank you for your comments. In section 5.1 of our revised manuscript, the uncertainty caused by using idealized core-shell model was discussed by replacing the BC core with cluster-like aggregates calculated with multiple sphere T-matrix (MSTM) method. The relative deviation between MAC calculated by MSTM model and by core-shell Mie model was investigated. The results showed that when the size of BC core was smaller than 150 nm, the overall deviation was within 4 %, which indicated that Mie theory was a good approximation to the BC aggregates even when BC core reached 200 nm. When BC core was larger than 200 nm, MAC calculated by MSTM model increased with increasing thickness of shell. The deviations between MAC calculated by the idealized concentric core-shell model and letting BC particles be in the form of

cluster-like aggregates were overall within 15%.

Specific comments:

1) Wavelength should be addressed when the absolute value of MAC is mentioned.

Response: Thank you for your recommendation. Wavelength was addressed when the absolute value of MAC was mentioned.

2) Line 13, what do the 'different core-shell structures' mean? Different core size and shell thickness?

Response: Yes, 'different core-shell structures' meant different core sizes and shell thicknesses in this study. 'Different core-shell structures' was changed into 'different core sizes and shell thicknesses' in the revised manuscript to avoid ambiguity.

3) Line 57–58, Bond and Bergstrom (2006) just suggested a consistent MAC for fresh (uncoated) BC particles.

Response: This sentence was removed in the revised manuscript.

4) Line 73, a more detailed but clear description of BCPMSD measurement should be addressed. From my understanding, major results and discussion presented in this study are based on the BCPMSD measurements (using DMA-AE51?) at Zhangqiu site. DMA-SP2 measurements at Taizhou, and comparisons of AE33 with PASS-3 at Taizhou and Beijing are mostly used to provide essential parameters (e.g., number fraction of BC-containing particles, multi-scattering correction factor for AE33, etc.) for the BCPMSD retrieval.

Response: Thanks for your comments. More detailed description of BCPMSD measurement was addressed in section 2.2 in our revised manuscript.

Yes, the major results and discussion in this study were based on BCPMSD measurements using DMA-AE51 at Zhangqiu site. The SP2 measurements at Taizhou

as well as comparison between AE33 and PASS-3 were used to provide number fraction of BC-containing particles as well as multi-scattering correction factor for AE33.

5) Line 112–115, the method to determine the size-resolved number fraction of BC-containing particles should be introduced briefly. How to deal with the effect of multicharged particles in the DMA-SP2 system? Why the number fraction of BC-containing particles at Taizhou can be used to represent that at Zhangqiu?

Response: Thanks for your recommendation. The determination of the number fraction of BC-containing particle was introduced briefly in the text.

According to the study of Zhao et al. (2019), The peak height (H) of the aerosol scattering signal could be used to deal with multicharged particle. The probability distribution of H at a given selected mobility diameter had multiple modes, as Fig. 1 showed. The multiple modes corresponded to signals of multicharged particles and could be calculated with theory of DMA.

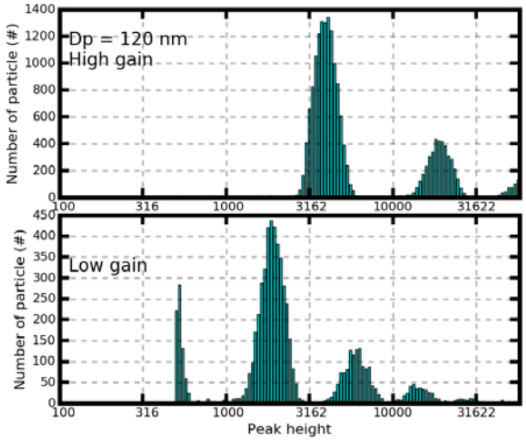

Figure 1. Figure S1 of the study by Zhao et al. (2019). The measured scattering signal distribution at diameter of 120 nm using ammonium sulfate.

Both Zhangqiu site (36°42’N, 117°30’E) and Taizhou site (32°35’N, 119°57’E) are in the east of China. They both experienced pollutions caused by industrialization and urbanization in the past several decades. Hence, the number fraction of BC-containing particle measured at Taizhou was representative and could be used as reference value for Zhangqiu.

6) Line 120, why absorption coefficients measured by AE33 are 2.9 times those measured by PASS-3? Does this ratio mean the multi-scattering effect of the filter loading method? However, as mention in line 106, a compensation factor of 2.6 has been introduced to mitigate multiple scattering effect. Was the PASS-3 well calibrated before the measurement?

Response: 2.9 was from the study by Zhao et al. (2020).

Yes, this ratio, namely the scattering correction factor, was used to correct multi-scattering effect.

In line 106, the factor of 2.6 was the scattering correction factor for AE51. And for AE33 was 2.9. We specified that 2.6 was for AE51.

7) Line 147, although the mantle chemical species would not influence largely the results presented in this study, BC/OM mixtures are more likely existed in the atmosphere of studied regions.

Response: Thanks for the comments. The wavelength used in this study was 880 nm. Previous study indicates aerosol absorption at 880 nm is mainly from BC (Ramachandran and Rajesh, 2007). Therefore, the influence of organic matter was neglected in this study.

References

Petzold, A., Ogren, J. A., Fiebig, M., Laj, P., Li, S. M., Baltensperger, U., Holzer-Popp, T., Kinne, S., Pappalardo, G., Sugimoto, N., Wehrli, C., Wiedensohler, A., and Zhang, X. Y.: Recommendations for reporting "black carbon" measurements, Atmospheric Chemistry and Physics, 13, 8365-8379, 10.5194/acp-13-8365-2013, 2013.

Ramachandran, S., and Rajesh, T. A.: Black carbon aerosol mass concentrations over Ahmedabad, an urban location in western India: Comparison with urban sites in Asia, Europe, Canada, and the United States, J. Geophys. Res.-Atmos., 112, 19, 10.1029/2006jd007488, 2007.

Zhao, G., Zhao, W. L., and Zhao, C. S.: Method to measure the size-resolved real part

of aerosol refractive index using differential mobility analyzer in tandem with single-particle soot photometer, Atmospheric Measurement Techniques, 12, 3541-3550, 10.5194/amt-12-3541-2019, 2019.

Zhao, G., Yu, Y., Tian, P., Li, J., Guo, S., and Zhao, C.: Evaluation and Correction of the Ambient Particle Spectral Light Absorption Measured Using a Filter-based Aethalometer, Aerosol and Air Quality Research, 20, 1833-1841, 10.4209/aaqr.2019.10.0500, 2020.

Response to Anonymous Referee #2

Major comments:

1) The authors have ignored the recommendations as proposed by Petzold et al. (2013), recommendations that are generally accepted by the scientific community, on how black carbon (BC) should be reported when derived from instruments that measure light attenuation, i.e. filter based or photoacoustic sensor. BC derived from these techniques should be reported as equivalent BC, or eBC. If or when this paper is resubmitted, the title should reflect clearly that it is eBC that is being discussed, not BC.

Response: Thanks for your recommendation. The term 'black carbon' (BC) was changed into 'equivalent BC'. As suggested by Petzold et al. (2013), equivalent BC was abbreviated to "EBC" in the revised manuscript.

2) A large fraction of the introduction is devoted to the importance of BC for climate change due to radiative forcing. What the authors fail to understand is that in the context of their study, the corrections to the MAC that they are proposing is completely irrelevant. Sensors that measure light absorption like the Aethalometer, are already providing the necessary information that is relevant to climate change, i.e. it is not the mass concentration that is important it is the optical cross section. I will address this further below with respect to the mixing state of BC, but the primary point is that the mass concentration of BC is not important when doing radiative transfer calculations if you already have the primary measurements of the coefficients of scattering and absorption. The authors also mention that BC might be efficient CCN or IN, both true statements but again irrelevant with respect to their study. Hence, the introduction needs to be completely rewritten to explain the real relevance of the current study, and that is to set some error bounds on eBC derived from Aethalometer measurements and NOT a cutting edge, new methodology that will in any way improve the accuracy of such measurements.

Response: Thank you for your comments. The introduction was rewritten to emphasize the importance of MAC correction when deriving EBC from light absorption based on filter-based instrument.

3) This study should be written up as a detailed analysis of the uncertainties in the MAC related to the mixing state of BC, i.e. the refractive indices, real and imaginary, the wavelength of incident light, and the relative sizes of the core and shell. Secondly, in the introduction, it should be made quite clear how this analysis differs from the many others that have already been published.

Response: Thank you for your comments. Detailed uncertainty analysis, including refractive indices, was input in section 5 of the revised manuscript. The discussions included uncertainties of MAC caused by using idealized core-shell model, using constant BC-containing particle fraction, and variation of RI. The influence of sizes of core and shell were discussed in the uncertainty analysis. With respect to wavelength, EBC is derived from σ_{ab} at a specific wavelength, namely 880 nm. At 880 nm, aerosol absorption is mainly from BC (Ramachandran and Rajesh, 2007). At shorter wavelength, absorption of organic carbon is not negligible any more, leading to difficulty of extracting BC absorption from total absorption. Therefore, the wavelength dependency of MAC was not discussed since the main goal of this study was to derive EBC, and the organic component was not included in this study.

The variation of MAC due to mixing state was not considered when deriving EBC from σ_{ab} in the previous studies, difference between this study and previous studies was input in the text. The motivation of this study was to propose a modified approach considering variation of MAC due to mixing state.

4) The methodology that is discussed in this paper is being promoted as a way to derive a more accurate EBC but this is misleading because in order to apply this you need a lot of additional complementary information about the size distribution of the BC, the fraction of particles that are mixed with BC, etc. If you had all the necessary information to begin with, then you wouldn't even need to try and derive EBC using

a variable MAC because you would already have enough information to estimate BC without the light absorption instrument. This should be made quite clear in a resubmission of this paper.

Response: Thank you and we agree with your comments. Filter based instruments such as AE33 are used in operational networks worldwide due to their advantages such as low cost, simplicity of operation, less maintenance and convenience for data processing. However, the EBC measured by AE33 is not accurate because it uses a constant MAC. The motivation of this study was to propose a method to consider the variation of MAC to make EBC measured by AE33 more accurate.

The size distribution of BC required in this study was size distribution of absorption measured by aethalometer, which could be achieve by DMA in tandem with AE51. As for the number fraction of particles mixed with BC (N_{BC}), it was a reference value in this study. Uncertainty analysis showed that derived EBC was not that sensitive to N_{BC}.

5) It is my opinion that the modeling that is being discussed with this study has as much importance for setting the error bars on light absorption derived from the filter-based measurements as for setting error bars for deriving eBC. There are many corrections that have been proposed to adjust the light absorption measurements for the impact of overloading, filter matrix effects, etc., but perhaps the results from the current study could also be used to establish how mixed state BC leads to under/over estimates of the absorption coefficient. The authors should give this serious consideration if they want their study to have more relevancy than it does in its current state.

Response: Thank you for your comments. As mentioned above, the filter-based instruments such as AE33 are widely used in operational networks due to their advantages. This study aimed to investigate the role of variation in MAC on the derived EBC by AE33. Besides correction to EBC, more discussions about the effect of mixing state on the absorption coefficient were input in the text.

Specific comments:

1) Line 1, "determination of black carbon mass concentration from aerosol light absorption using variable mass absorption cross-section". Here and from here on out this is to be called "equivalent black carbon".

Response: "Black carbon" was changed into "equivalent black carbon" in the text.

2) Line 10, "the mass absorption cross-section (MAC) is a crucial parameter for converting light absorption coefficient (σ_{ab}) to mass equivalent BC concentration (m_{BC})". Here and forward, change this into eBC.

Response: m_{BC} was modified as EBC in the revised manuscript here and forward.

3) Line 11, "traditional filter-based instrument, such as AE33, uses a constant MAC of 7.77 m^2/g to derive m_{BC}, which may lead to uncertainty in m_{BC}." Add the wavelength that this is for.

Response: Thanks for your recommendation. wavelength of 880 nm was appended to 7.77 m^2/g in the text.

4) Line 22, "because of its highly absorbing properties in the visible spectral region, BC is considered to have a significant influence on global warming." By definition, "black" means all wavelengths, not just visible.

Response: "In the visible spectral region" was deleted in the revised manuscript.

5) Line25, "despite the importance of BC to climate, the global mean direct radiative forcing of BC particles still spans over a poorly constrained range of 0.2 – 1 W/m^2." Please clarify. I don't understand what this means.

Response: This sentence was removed from the text to avoid ambiguity.

6) Line 29, "to fully evaluate the influences of BC particles on solar radiation or

precipitation, more precise measurements of BC mass loading in the atmosphere are required." This is an incorrect argument for saying that more accurate measurements of BC are needed because instrument like the aethalometer measure light absorption directly without the need for converting it to eBC. With respect to the impact on clouds, what is needed is better measurements that can show just exactly how BC does form droplets or ice. Hence, an accurate MAC is not relevant for these impacts. The only impact that BC mass has that is important is on health or damage to building surfaces.

Response: Thanks for your comments. This sentence was deleted in the revised manuscript to make the content more relevant to the correction to EBC.

7) Line 31, "a variety of techniques have been developed to measure real-time BC mass concentrations." None of these measure BC mass concentrations.

Response: These absorption measurement techniques was removed and instruments measuring BC mass concentration, such as SP2, OCEC, SP-AMS, was input in the text.

8) Line 37 and line 38, "it measures real-time BC concentrations by converting the absorption coefficient (σ_{ab}) into mass equivalent BC concentrations (m_{BC}) through a constant mass absorption cross-section (MAC), which provides the BC absorption per unit mass." AE33 does not measure BC concentrations and the wavelength dependency of MAC has to be discussed at the very beginning.

Response: "BC concentrations" was changed into "BC absorption" and "880 nm" was appended to MAC.

8) Line 53, "a wide range of MAC (2 – 25 m^2/g) has been reported in previous studies." This range is due to wavelength dependency. What is the range for a single frequency, especially for the one being used here?

Response: Thanks for your comments. This sentence was changed into "A wide range of MAC has been reported in previous studies. For instance, Bond and Bergstrom (2006) reported MAC at 550 nm varying from 1.6 m^2/g. Sharma et al. (2002) reported MAC

at 880 nm varying from 6.4 to 28.3 m^2/g." to make wavelength dependency clear.

9) Line 62 to 64, "the hypothetical BC mixing state affects the corresponding absorption properties. It is critical to propose a method to infer m_{BC} from light attenuation measurements considering aerosol size and the process by which BC aerosols mix with other aerosol components." Is this being proposed, completely independent of any other information about the environment?

Response: The mixing state of BC was one of the important factors that affect the absorption properties of BC-containing particles. The size of aerosol was required to estimate the effect of mixing state on BC absorption. It was dependent on other information, such as refractive index (RI). The influence of RI on the uncertainty of MAC was discussed in the later content. This sentence was removed to avoid ambiguity.

10) Line 70, "this modified method measures size-resolved m_{BC} accurately and improves the evaluation of BC radiative forcing." How can a theoretical model "measure" eBC?

Response: Thanks for your comment. "Measure" was modified into "estimate".

11) Line 77, "the DMA (Differential Mobility Analyzer)-SP2 system measurements to determine the number fraction of BC-containing aerosols and to compare <u>AE33</u> and the three-wavelength photoacoustic soot spectrometer (PASS-3) were conducted in Taizhou." What wavelength of AE33 are compared?

Response: The wavelengths used for comparison between AE33 and PASS-3 were 405 nm, 532 nm and 781 nm. 405 nm, 532 nm and 781 nm are the wavelengths PASS-3 measures. The wavelengths AE33 measures are 370 nm, 470 nm, 520 nm, 590 nm, 660 nm, 880 nm and 950 nm. For AE33, 405 nm, 532 nm and 781 nm were calculated with wavelengths pairs of (370 nm, 470 nm), (520 nm, 590 nm) and (660 nm, 880 nm) through Ångström relationship:

$$\frac{\sigma_{\mathrm{ab}}(\lambda_1)}{\sigma_{\mathrm{ab}}(\lambda_2)} = \left(\frac{\lambda_1}{\lambda_2}\right)^{-\alpha_{ab}},$$

$$\sigma_{\mathrm{ab}}(\lambda) = \sigma_{\mathrm{ab}}(\lambda_1)\left(\frac{\lambda}{\lambda_1}\right)^{-\alpha_{ab}}.$$

Detailed description can be found in (Zhao et al., 2020). Wavelengths (405 nm, 532 nm and 781 nm) as well as the reference was appended to the manuscript.

12) Line 84, "Meanwhile, from March 21, 2017 to April 9, 2017 at the Peking University site, the results from simultaneous measurements from AE51 (model 51, microAeth, USA) and AE33 were compared." What wavelength?

Response: The wavelength of AE51 was 880 nm. Wavelength of "880 nm" was appended to "AE51 and AE33".

13) Line 99, "the dry aerosol scattering coefficients at 525 nm were measured simultaneously by an integrated nephelometer (Ecotech 100 Pty Ltd., Aurora 3000) with a flow rate of 3 L/min." How does this wavelength correspond to the Aethalometer wavelengths?

Response: The dry scattering coefficient at 525 nm here was used as a proxy of pollution level. At a specific wavelength, higher (lower) dry scattering coefficient could indicate a relatively polluted (clean) episode. Dry scattering coefficient at 525 nm was not used for comparison with light attenuation measured by aethalometer. "As an indicator of pollution level" was appended to the sentence.

14) Line 105, "factor k was set as 0.004 and ATN is the measured light attenuation when particles load on the fiber filter of AE51." Where does this value come from?

Response: "k = 0.004" was from the work by Zhao et al. (2019). "(Zhao et al., 2019b)" was appended to "0.004" in the manuscript.

15) Line 114 – 115, "according to the measurements from Taizhou, only 17% of the ambient particles that contained BC averagely for bulk aerosol populations." This is

an incomplete sentence.

Response: this sentence was modified into “according to the measurements from Taizhou, only 17% of the ambient particles contained BC averagely for bulk aerosol populations.”.

16) Line 116, “we adjusted the measured wavelengths of AE33 to the measured wavelengths of PASS-3 (405 nm, 532 nm, and 781 nm).” How the adjustment is made?

Response: 405 nm, 532 nm and 781 nm are the wavelengths PASS-3 measures. The wavelengths AE33 measures are 370 nm, 470 nm, 520 nm, 590 nm, 660 nm, 880 nm and 950 nm. They are not consistent. For comparison, the wavelengths of AE33 were interpolated to the wavelengths of PASS-3 in this study. Specifically, For AE33, 405 nm, 532 nm and 781 nm were interpolated with wavelengths pairs of (370 nm, 470 nm), (520 nm, 590 nm) and (660 nm, 880 nm) through Ångström relationship:

$$\frac{\sigma_{\mathrm{ab}}(\lambda_1)}{\sigma_{\mathrm{ab}}(\lambda_2)} = \left(\frac{\lambda_1}{\lambda_2}\right)^{-\alpha_{\mathrm{ab}}},$$

$$\sigma_{\mathrm{ab}}(\lambda) = \sigma_{\mathrm{ab}}(\lambda_1)\left(\frac{\lambda}{\lambda_1}\right)^{-\alpha_{\mathrm{ab}}}.$$

More detailed description could be found in (Zhao et al., 2020). The interpolation method was added to the manuscript. “Adjusted” was changed into “interpolated”.

17) Line 182 – 183, “it should be pointed out that the retrieval algorithm of BCPMSD is based on the assumption that BC-containing particles of a fixed diameter are all core-shell mixed and the corresponding D_{BC} for a specific $D_{particle}$ is same.” A major assumption. Where is the sensitivity study that evaluates this assumption? This uncertainty analysis belongs in the main text, not in a supplement.

Response: Thanks for your comments. The sensitivity study from the supplement was moved to the section 5.1 in the revised manuscript.

Reference

Petzold, A., Ogren, J. A., Fiebig, M., Laj, P., Li, S. M., Baltensperger, U., Holzer-Popp,

T., Kinne, S., Pappalardo, G., Sugimoto, N., Wehrli, C., Wiedensohler, A., and Zhang, X. Y.: Recommendations for reporting "black carbon" measurements, Atmospheric Chemistry and Physics, 13, 8365-8379, 10.5194/acp-13-8365-2013, 2013.

Ramachandran, S., and Rajesh, T. A.: Black carbon aerosol mass concentrations over Ahmedabad, an urban location in western India: Comparison with urban sites in Asia, Europe, Canada, and the United States, J. Geophys. Res.-Atmos., 112, 19, 10.1029/2006jd007488, 2007.

Zhao, G., Tao, J. C., Kuang, Y., Shen, C. Y., Yu, Y. L., and Zhao, C. S.: Role of black carbon mass size distribution in the direct aerosol radiative forcing, Atmospheric Chemistry and Physics, 19, 13175-13188, 10.5194/acp-19-13175-2019, 2019.

Zhao, G., Yu, Y., Tian, P., Li, J., Guo, S., and Zhao, C.: Evaluation and Correction of the Ambient Particle Spectral Light Absorption Measured Using a Filter-based Aethalometer, Aerosol and Air Quality Research, 20, 10.4209/aaqr.2019.10.0500, 2020.

Response to Anonymous Referee #3

Major comments:

1) As the authors pointed, for the new BC, its shape is chain-like, not a spherical one, so how do you know this method is applicable for the measurement. How many parts of BC is newly generated and how many is old one is there a guess for that? Do you have some samples measured ASAP and others saved and wait some time to let them to be old one?

Response: Thank you very much for your comments. We discussed the uncertainties caused by using idealized core-shell model in section 5 of our new manuscript. We replaced the spherical BC particle with cluster-like aggregates using multiple sphere T-matrix (MSTM) method. The results show that the deviations between the idealized concentric core-shell model and the cluster-like aggregates are overall within 15%. For BC core smaller than 200 nm, the deviations are within 4%. So, the method is applicable for the measurement.

After emitted into ambient environment, a pure BC particle will soon be coated. The absorption ability of the coated BC particle will be enhanced due to lensing effect. the absorption coefficient (σ_{ab}) of the coated BC particle will be larger that of pure BC particle. In our method, we do not limit the BC-containing particle that it has to be core-shell structure, it can also be a pure BC particle as long as the calculated σ_{ab} matches measured σ_{ab}. So, we do not need to guess how many parts of BC is newly generated and how many parts of BC is old.

Sorry, we do not have sample measured ASAP and others saved and wait some time to let them to be old one. But according to the work of Peng et al. (2016), the aging time scale is ~ 4 hours.

Specific comments:

1) Line 16, "with in" should be "within".

Response: We changed “with in” into “within” in our new manuscript.

2) Line 58, what’s mean of “degree of MAC”?

Response: “The degree of MAC” actually means “the value of MAC”. We changed “the degree of MAC” into “the value of MAC” in our new manuscript to avoid ambiguity.

3) “… Mie model incorporated with core-shell configuration hypothesis was applied in this study to assess the limitation of the constant …” should be simplified as “… Mie model with assumption of core-shell particles was …”

Response: We changed “… Mie model incorporated with core-shell configuration hypothesis was …” into “… Mie model with assumption of core-shell particles was …” in our new manuscript.

4) Line 68, “Based on the detailed…” The word “the” should be deleted.

Response: we removed “the” in our new manuscript.

5) Line 73, “The measured BC particle mass size distribution (BCPMSD) was obtained from the field campaign conducted at the Zhangqiu Meteorology Station (36°42’N, 117°30’E), Shandong Province. This field campaign lasted for about 1 month, from July 23, 2017 to August 24, 2017. The Zhangqiu observation site is located in the North China Plain (NCP) and is surrounded by farmland and residential areas, representing regional background conditions of the NCP.” should be rewritten as “The BC particle mass size distribution (BCPMSD) was measured at Zhangqiu Meteorology Station (36°42’N, 117°30’E), Shandong Province, surrounded by farmland and residential areas and a typical site for regional background conditions of North China Plain (NCP). The field campaign lasted for about 1 month, from July 23, 2017 to August 24, 2017.”

Response: We changed this part into “The BC particle mass size distribution (BCPMSD) was measured at Zhangqiu Meteorology Station (36°42’N, 117°30’E), Shandong Province, surrounded by farmland and residential areas and a typical site for regional

background conditions of North China Plain (NCP). The field campaign lasted for about 1 month, from July 23, 2017 to August 24, 2017." in our new manuscript.

6) Line 76, the last word "system" should be deleted.

Response: We deleted "system" in our new manuscript.

7) Line 77, "measurements to determine …" should be "is used to determine …".

Response: We changed "measurements to determine …" into "is used to determine …" in our new manuscript.

8) Line 78, "The suburban measurement site", the word "measurement" should be deleted.

Response: We deleted the "measurement" in our new manuscript.

9) Line 79, the word "the" before "Jianghuai Plain" should be deleted.

Response: We deleted "the" before "Jianghuai Plain" in our new manuscript.

10) Line 86 and 87, "All the measurements in the three sites were conducted in containers where ambient temperature was controlled within 24 ± 2 °C with a particle pre-impactor to remove particles larger than 10 μm from the input air stream." should be rewritten as "All the measurements in the three sites were conducted in temperature (24 ± 2 °C) controlled containers, and a particle pre-impactor is used to remove particles larger than 10 μm from the input airflow."

Response: The sentence was changed into "All the measurements in the three sites were conducted in temperature (24 ± 2 °C) controlled containers, and a particle pre-impactor is used to remove particles larger than 10 μm from the input airflow." In our new manuscript.

11) Line 92, "developed by (Ning et al., 2013). The instrument setup was further improved by Zhao et al. (2019b)." should be "developed by Ning et al. (2013) and

improved by Zhao et al. (2019b)".

Response: we changed "developed by (Ning et al., 2013). The instrument setup was further improved by Zhao et al. (2019b)" into "developed by Ning et al. (2013) and improved by Zhao et al. (2019b)" in our new manuscript.

12) Line 101, "that were used to represent air pollution conditions" should be deleted.

Response: "that were used to represent air pollution conditions" was deleted in our new manuscript.

13) Line 105, the variables of k and ATN should be italic.

Response: k and ATN were changed into italic in our new manuscript.

14) Line 108, "in this study" should be deleted.

Response: "in this study" was deleted in our new manuscript.

15) Beginning of line 115, word "from" should be "at" and the same for line 117.

Response: "from" was changed into "at" in our new manuscript.

16) Line 117 and 118, "with a measurement flowrate of" should be "with flowrate of".

Response: "with a measurement flowrate of" was changed into "with flowrate of" in our new manuscript.

17) Line 123, "… through a constant MAC value" should be "under assumption of a constant MAC".

Response: "… through a constant MAC value" was changed into "under assumption of a constant MAC".

18) Line 130, "an appropriate model simulation is needed for representing a single BC particle's optical properties." What's meaning of this sentence?

Response: This sentence means that a proper model is required to simulate the optical parameters, such as the MAC, absorption coefficient, and scattering coefficient, of BC-containing particles to a good approximation. To avoid ambiguity, this sentence was changed into "a proper model is required to simulate the optical properties of BC-containing particles to a good approximation." in our new manuscript.

19) Line 131, "There are three widely employed mixing states that are used to represent the structure of BC-containing aerosols" should be "Three widely employed mixing states are used to represent the structure of BC-carried aerosols".

Response: The sentence was changed into "Three widely employed mixing states are used to represent the structure of BC-carried aerosols." in our new manuscript.

20) Line 133, "… chain-like aggregates composed of small spheres" should be "chain-like aggregates of small spheres".

Response: "chain-like aggregates composed of small spheres" was changed into "chain-like aggregates of small spheres" in our new manuscript.

21) Line 139, "the spherical core and shell favor the Mie model" should be deleted.

Response: "the spherical core and shell favor the Mie model" was deleted in our new manuscript.

22) Line 140, "in this study" should be deleted.

Response: "in this study" at line 140 was deleted in our new manuscript.

23) Line 143, could you use other words for the section title?

Response: The section title was changed to "Simulation of MAC for BC-containing particle using Mie theory".

24) Line 147, the word "frequent" should be replace by "common".

Response: the word "frequent" was replaced by "common" in our new manuscript.

25) Line 150, "… at the wavelength of 880 nm, calculated using the Mie theory, has been presented" should be "… at wavelength of 880 nm are simulated with Mie scattering method."

Response: "… at the wavelength of 880 nm, calculated using the Mie theory, has been presented" was changed into "… at wavelength of 880 nm are simulated with Mie scattering method." in our new manuscript.

26) Line 151, "reported to vary with incident light wavelength" should be "dependent on light wavelength".

Response: "reported to vary with incident light wavelength" was changed into "dependent on light wavelength" in our new manuscript.

27) Line 152~153, "as BC particles can be emitted from different fuels and conditions, RI cannot be observed directly, with both real and imaginary part of RI varying over a significantly wide range" should be "due to different sources of BC, both the real and imaginary part of RI varies over a significantly wide range".

Response: "as BC particles can be emitted from different fuels and conditions, RI cannot be observed directly, with both real and imaginary part of RI varying over a significantly wide range" was changed into "due to different sources of BC, both the real and imaginary part of RI varies over a significantly wide range" in our new manuscript.

28) Line 157, "averaged values are illustrated …" Do you mean "mean values …"

Response: Yes, "averaged values" are actually "mean values". To avoid ambiguity, "averaged values" was changed into "mean values" in our new manuscript.

29) Please rewrite paragraph between line 168 and 173 to make it simple and clear.

Response: The paragraph between line 168 and 173 was rewritten to make it simpler and clearer in our new manuscript.

30) Line 174, the first sentence "The detailed iterative procedure is illustrated in Fig. 2." Should be reposition to the end of last paragraph, and the word "detailed" should be "deleted".

Response: The first sentence at Line 174 was repositioned to the end of the paragraph and the word "detailed" was deleted in our new manuscript.

31) Line 175, "represented" should be replace by "shown".

Response: "represented" was replace by "shown" in our new manuscript.

32) Line 175, "a simplified algorithm for deriving BCPMSD was proposed by considering Fig. 1 as a look-up table." Should be rewritten as "a simplified algorithm was proposed to derive BCPMSD through a pre-calculated look-up table."

Response: "a simplified algorithm for deriving BCPMSD was proposed by considering Fig. 1 as a look-up table." was rewritten as "a simplified algorithm was proposed to derive BCPMSD through a pre-calculated look-up table." in our new manuscript.

33) Line 195 and 196, words "finer mode" and "coarser mode" should be replaced by "fine mode" and "coarse mode", please read through the whole draft to replace other similar words.

Response: "finer mode" and "coarser mode" was replaced by "fine mode" and "coarse mode" through the whole draft in our new manuscript.

34) Line 198, "The results indicate that with the boundary of 280 nm, two opposite deviation tendencies exist." should be replaced by "the results show that there exist two opposite deviation trends before and after the turning point around 280nm."

Response: "The results indicate that with the boundary of 280 nm, two opposite deviation tendencies exist." was replaced by "the results show that there exist two opposite deviation trends before and after the turning point around 280nm." in our new manuscript.

35) Line 247, "The variations in on …" should be "The variation of …"

Response: "The variations in on …" was changed into "The variation of …" in our new manuscript.

36) Line 247, "all MACs in the look-up table in Fig. 1 are the mean values as the imaginary part and real part of BC RI varied over a wide range." What's the meaning of this sentence mean, please rewrite?

Response: This sentence was rewritten as "for a MAC (880 nm) point at ($D_{particle}$, D_{BC}) of Fig. 1, it is actually a mean value averaged with respect to both real part of RI varied from 1.5 to 2.0 and imaginary part of RI varied from 0.5 to 1.1." in our new manuscript.

37) Please rewrite the whole paragraph between line 247~260 to make it clear and simple.

Response: the whole paragraph between line 247~260 was re written in our new manuscript to make it clear and simple.

38) Line 454 to line 459, please rewrite caption for Figure 3 and make it easy to read. The same for the caption of Figure 4.

Response: The captions for Fig. 3 and Fig. 4 were rewritten in our new manuscript to make it easy to read.

Peng, J. F., Hu, M., Guo, S., Du, Z. F., Zheng, J., Shang, D. J., Zamora, M. L., Zeng, L. M., Shao, M., Wu, Y. S., Zheng, J., Wang, Y., Glen, C. R., Collins, D. R., Molina, M. J., and Zhang, R. Y.: Markedly enhanced absorption and direct radiative forcing of black carbon under polluted urban environments, Proceedings of the National Academy of Sciences of the United States of America, 113, 4266-4271, 10.1073/pnas.1602310113, 2016.

Determination of equivalent black carbon mass concentration from aerosol light absorption using variable mass absorption cross-section

Weilun Zhao[1], Wangshu Tan[1,2], Gang Zhao[1,2,3], Chuanyang Shen[1], Yingli Yu[4,1], Chunsheng Zhao[1]

[1]Department of Atmospheric and Oceanic Sciences, School of Physics, Peking University, Beijing 100871, China

[2]School of Optics and Photonics, Beijing Institute of Technology, Beijing 100081, China

[2]State [3]State Key Joint Laboratory of Environmental Simulation and Pollution Control, College of Environmental Sciences and Engineering, Peking University, Beijing 100871, China

[4]Economics & Technology Research Institute, China National Petroleum Corporation, Beijing 100724, China

Correspondence to: Chunsheng Zhao (zcs@pku.edu.cn)

Abstract. Atmospheric black carbon (BC) is the strongest visible solar radiative absorber in the atmosphere, exerting significant influences on the earth's radiation budget. The mass absorption cross-section (MAC) is a crucial parameter for converting light absorption coefficient (σ_{ab}) to mass equivalent BC mass concentration (EBCm_{BC}). Traditional filter-based instrument, such as AE33, uses a constant MAC of 7.77 m^2/g at 880 nm to derive m_{BC}EBC, which may lead to uncertainty in m_{BC}EBC. In this paper, a new method of converting σ_{ab} to m_{BC} EBC is proposed by incorporating the variations of MAC attributed to the influences of aerosol coating state. Mie simulation showed that MAC varied dramatically with different core-shell structurescore sizes and shell thicknesses. We compared our new method with traditional method during a field measurement at a site of North China Plain. The results showed that the MAC at 880 nm was smaller (larger) than 7.77 m^2/g for particle smaller (larger) than 280 nm, resulting in BCEBC mass size distribution derived from new method was higher (lower) than traditional method for particle smaller (larger) than 280 nm. Size-integrated BCEBC mass concentration derived from the new method was 16% higher than traditional method. Sensitivity analysis indicated that the uncertainty in EBCm_{BC} caused by refractive index (RI) was with in 35% and the imaginary part of RI had dominant influence on the derived EBCm_{BC}. This study emphasizes the necessity to take variations of MAC into account when deriving EBCm_{BC} from σ_{ab} and can help constrain the uncertainty in m_{BC} EBC measurements.

1 Introduction

Black carbon (BC) is an important component of ambient aerosol particles. Because of its highly absorbing properties in the visible spectral region, BC is considered to have a significant influence on global warming. The warming effects of BC is only second to that of carbon dioxide (Ramanathan and Carmichael, 2008). Despite the importance of BC to climate, the global mean direct radiative forcing of BC particles still spans over a poorly constrained range of 0.2 – 1 W/m^2 (Chung et al., 2012;Bond et al., 2013;Boucher et al., 2013). The large uncertainty of BC radiative forcing is partially attributed to the lack of reliable measurements of BC mass concentration in the atmosphere (Arnott et al., 2005;Boucher et al., 2013). Furthermore, BC aerosols can serve as cloud condensation nuclei or ice nucleation particles and change atmospheric convection by heating aerosol layer and influencing the regional precipitation patterns and cloud lifetime. To fully evaluate the influences of BC particles on solar radiation or precipitation, more precise measurements of BC mass loading in the atmosphere are required.

带格式的: 缩进: 首行缩进: 0 厘米

带格式的: 上标

带格式的: 上标

A variety of techniques have been developed to measure real-time BC mass concentrations. Aethalometer (Hansen et al., 1984), Particle Soot Absorption Photometer (PSAP) (Bond et al., 1999), and Multiple-Angle Absorption Photometer (MAAP) (Petzold and Schonlinner, 2004) are based on filter-based attenuation, while the Single Particle Soot Photometer (SP2) is a light-induced incandescent instrument . Other instruments that use photo-acoustic methods such as Photoacoustic Spectrometer (PAS) (Truex and Anderson, 1979) or Photo-Acoustic Soot Spectrometer (PASS) have also been introduced. The aethalometer AE33 (model 33, Magee, USA), a convenient and rapid instrument, is commonly used for routine BC observations or dedicated campaigns (Castagna et al., 2019;Sandradewi et al., 2008;Helin et al., 2018). It measures real-time BC concentrations by converting the absorption coefficient (σ_{ab}) into mass equivalent BC concentrations (m_{BC}) through a constant mass absorption cross-section (MAC), which provides the BC absorption per unit mass.

However, it has been reported that the MAC of BC is substantially affected by the process through which BC mixes with other aerosol components (Gunter et al., 1993;Doran et al., 2007;Lack and Cappa, 2010;Peng et al., 2016). Field measurements have indicated that fresh BC particles are generally subject to several coating processes while being transported in the atmosphere and tend to be covered in layers of other organic or inorganic components (Shiraiwa et al., 2007;Cappa et al., 2019;Bond et al., 2006). The gathered shell that builds up on the BC core, acting as a lens to focus additional incident light on the enclosed BC core, can enhance BC light absorption (Fuller et al., 1999) and has significant influences on the BC radiative forcing (Jacobson, 2001). This light absorption enhancement has been termed as "lensing effect" of the BC particles.

For typical core-coating mixed BC containing particles, this lensing effect was found to enhance BC absorption by 50-100% (Bond et al., 2006). Schwarz et al. (2008) found that fresh soot particles internally mixed with sulfates and organics during transportation, and the lensing effect enhanced the light absorption by a factor of 1.3-1.5. Some controlled laboratory studies also confirmed the occurrence of absorption enhancement and their conclusions were consistent with the model calculation (Adler et al., 2010;Brem et al., 2012;Shiraiwa et al., 2010). Meanwhile, other field studies demonstrated a wide range of this lensing effect (Cappa et al., 2019). In contrast, some field observations showed a slight absorption enhancement (Cappa et al., 2012;Nakayama et al., 2014). A wide range of MAC (2-25 m^2/g) has been reported in previous studiesBond and Bergstrom (2006);Sharma et al. (2002)–

Some studies suggested using site-specific MAC values for converting σ_{ab} into m_{BC} (Martins et al., 1998;Schmid et al., 2006). However, field measurements indicated that MAC showed both large temporal and spatial variability (Bond and Bergstrom, 2006;Lack et al., 2012;Cappa et al., 2012;Ram and Sarin, 2009). Bond and Bergstrom (2006) suggested using consistent MAC and refractive index (RI) values for the BC measurements. In addition to the mixing state, the degree of MAC also relies on diameter of the BC core (D_{BC}), RI, coating thickness, and the location of the BC core (Bond and Bergstrom, 2006;Fuller et al., 1999;Lack and Cappa, 2010). To better determine the current atmospheric BC mass loading, a more reliable MAC application is imperative to infer BC mass from measured light attenuation.

The hypothetical BC mixing state affects the corresponding absorption properties. It is critical to propose a method to infer m_{BC} from light attenuation measurements considering aerosol size and the process by which BC aerosols mix with other aerosol components. A simplified core-shell configuration has been introduced to illustrate the structure of BC-containing particles and

带格式的: 缩进: 右侧: -0 厘米, 左 -0.01 字符, 定义网格后自动调整右缩进, 调整中文与西文文字的间距, 调整中文与数字的间距

带格式的: 缩进: 左 -0.01 字符

~~calculate the relevant optical properties. Several studies have demonstrated that it is appropriate to use the core-shell configuration for aged aerosol (Majdi et al., 2020;Liu et al., 2019;Li et al., 2019).~~

~~With the objective of improving the reliability of m_{BC} inferred from AE33, the Mie model incorporated with core-shell configuration hypothesis was applied in this study to assess the limitation of the constant conversion factor used for MAC. Based on the detailed analysis of the relationship among MAC, D_{BC}, and coating thickness (T_{shell}), a modified approach has been proposed for filter-based instruments to derive m_{BC} from σ_{ab}. This modified method measures size-resolved m_{BC} accurately and improves the evaluation of BC radiative forcing.~~

Black carbon (BC) is an important component of atmospheric aerosol particles. The warming effect of BC is only second to that of carbon dioxide (CO_2) (Ramanathan and Carmichael, 2008) because of its highly absorbing property. The environmental effect of BC is nonnegligible. The absorption of BC can significantly reduce visibility (Moosmuller et al., 2009). BC are considered a major factor of adverse health disease (Highwood and Kinnersley, 2006). The fractal aggregates morphology of BC provides substantial surface area for deposition of cancerogenic matter. The insoluble nature and fine size of BC make it deposit in the lung for a long time. Because the significant impact of BC, extensive measurement has been made to monitor atmospheric loading of BC and give reference to policymaker for mitigation.

The BC mass concentration (m_{BC}) is one of the important variables for BC measurement (Bond et al., 2013). Many methods have been proposed to determine m_{BC}. For instance, the single-particle soot photometer (SP2) measure refractory BC (rBC) based on laser-induced incandescence (Schwarz et al., 2006). The organic carbon/elemental carbon (OCEC) analyzer determines elemental carbon (EC) through heating collected sample in a subsequent helium/oxygen environment (Wu et al., 2012). Soot particle aerosol mass spectrometry (SP-AMS) combines laser-induced incandescence as well as laser vaporization used in mass spectrometry (Onasch et al., 2012) and also reports m_{BC} as rBC. However, the abovementioned instruments are complicated in structure, highly expensive, hard to maintain, and as a result, not widely used.

Filter-based instruments, such as aethalometer (Hansen et al., 1984), are commonly used for routine BC observations and dedicated campaigns (Castagna et al., 2019;Sandradewi et al., 2008;Helin et al., 2018) because they are convenient and easy to maintain. Aethalometer does not directly measure m_{BC} and actually measures light absorption. Aethalometer converts absorption coefficient (σ_{ab}) at 880 nm to equivalent BC mass concentration (EBC) (Petzold et al., 2013) through a fixed mass absorption cross-section (MAC, 7.77 m^2/g at 880 nm). However, field measurements indicated that MAC showed both large temporal and spatial variability (Bond and Bergstrom, 2006;Lack et al., 2012;Cappa et al., 2012). For example, Bond et al. (2006) reported MAC at 550 nm varying from 1.6 to 15.9 m^2/g. Sharma et al. (2002) reported MAC at 880 nm varying from 6.4 to 28.3 m^2/g. It is not appropriate to use a fixed MAC at when EBC is derived from σ_{ab} at 880 nm. The variation of MAC has to be taken into account to reduce the uncertainty in the σ_{ab}-derived EBC.

The mixing state of BC is one of the crucial reasons leading to large variation in MAC. Field measurements have indicated that fresh BC particles are generally subject to several coating processes while being transported in the atmosphere and tend to be covered in layers of other organic or inorganic components (Shiraiwa et al., 2007;Cappa et al., 2019;Bond et al., 2006). The gathered shell

that builds up on the BC core, acting as a lens to focus additional incident light on the enclosed BC core, can enhance BC light absorption (Fuller et al., 1999). As a result, a coated BC particle will have a bigger MAC than the original pure BC particle. This light absorption enhancement is termed as "lensing effect" of the BC-containing particles. For typical core-coating mixed BC-containing particles, this lensing effect was found to enhance BC absorption by 50-100% (Bond et al., 2006). Schwarz et al. (2008) found that fresh soot particles internally mixed with sulfates and organics during transportation, and the lensing effect enhanced the light absorption by a factor of 1.3-1.5.

At a given wavelength, such as 880 nm, the degree of MAC relies on the size and the location of BC core, coating thickness, as well as refractive index (RI) (Fuller et al., 1999;Lack and Cappa, 2010). A simplified core-shell configuration has been introduced to illustrate the structure of BC-containing particles and calculate the relevant optical properties. Several studies have demonstrated that it is appropriate to use the core-shell configuration for aged aerosol (Majdi et al., 2020;Liu et al., 2019;Li et al., 2019).

In the previous studies (Zhao et al., 2019b;Ran et al., 2016a;Ran et al., 2016b;Castagna et al., 2019), the variation of MAC due to mixing state was not considered when deriving EBC from σ_{ab}. With the objective of improving the reliability of σ_{ab}-derived EBC, the Mie model incorporated with core-shell configuration hypothesis was applied in this study to assess the limitation of fixed MAC on σ_{ab}-derived EBC. Based on the detailed analysis of the relationship among MAC, D_{BC}, and coating thickness (T_{shell}), a modified approach considering variation of MAC due to mixing state was proposed for filter-based instruments to derive EBC from σ_{ab}. Detailed uncertainty analysis is carried out to assess the influence of assumptions used in this study. This modified method estimates size-resolvoled EBC accurately and reduces the uncertainty in σ_{ab}-derived EBC with respect to mixing state.

2 Dataset and instrumentation

2.1 Measurement sites

~~The measured BC particle mass size distribution (BCPMSD)~~The EBC particle mass size distribution (BCPMSD) was ~~obtained~~ obtained ~~from the field campaign conducted~~ at the Zhangqiu Meteorology Station (36°42'N, 117°30'E), Shandong Province, surrounded by farmland and residential areas and a typical site for regional background conditions of North China Plain (NCP). ~~This~~ The field campaign lasted for about 1 month, from July 23, 2017 to August 24, 2017. ~~The Zhangqiu observation site is located in the North China Plain (NCP) and is surrounded by farmland and residential areas, representing regional background conditions of the NCP.~~

The number fraction of BC-containing aerosol (N_{BC}) is required during conversion from absorption to EBC. N_{BC} was not measured simultaneously at Zhangqiu due to limitation in instruments. N_{BC} is a reference value in this work and referred from measurement at Taizhou (32°35'N, 119°57'E). An SP2 was used to determine N_{BC} at Taizhou from May 24, 2018 to June 18, 2018. The suburban ~~measurement~~ site Taizhou lies at the south end of ~~the~~ Jianghuai Plain in the East of China. This industrial area between the two megacities of Nanjing and Shanghai has experienced severe pollution during the past thirty years. Hence, N_{BC} measured at Taizhou is representative and the campaign averaged N_{BC} is used in this work. ~~The measurements were conducted from May 24, 2018 to June 18, 2018. The DMA (Differential Mobility Analyzer) SP2 system measurement of the number fraction of BC-containing aerosols and~~ Besides, comparison between AE33 and the three-wavelength photoacoustic soot spectrometer (PASS-3) at 405 nm,

带格式的: 缩进: 左 -0.01 字符
带格式的: 字体: 加粗
带格式的: 下标
带格式的: 下标
带格式的: 下标
带格式的: 上标
带格式的: 非上标/ 下标
带格式的: 下标
带格式的: 下标

532 nm and 781 nm (Zhao et al., 2020) was also carried out at Taizhou for scattering correction of AE33.~~were conducted in Taizhou (119°57' E, 32°35' N). The suburban measurement site Taizhou lies at the south end of the Jianghuai Plain in the East of China. This industrial area between the two megacities of Nanjing and Shanghai has experienced severe pollution during the past thirty years. The measurements were conducted from May 24, 2018 to June 18, 2018.~~

Besides Taizhou, ~~The~~ the ~~measurements for comparing AE33 and PASS-3 were~~ comparison between AE33 and PASS-3 was also conducted from March 20, 2018 to April 30, 2018 and from October 10, 2018 to October 19, 2018 in Peking University (39°59'~~-~~N, 116°18'~~-~~E). This site is located at the northwest of Beijing, a megacity experiencing severe and complex urban pollution. ~~Meanwhile, f~~From March 21, 2017 to April 9, 2017 at the Peking University site, ~~the results from simultaneous measurements from~~ simultaneous measurements of aethalometer AE51 (model 51, microAeth, USA) and AE33 at 880 nm were carried out ~~compared~~to investigate the consistency between AE51 and AE33.~~-~~

2.2 Instruments

All the measurements in the three sites were conducted in temperature (24 ± 2 °C) controlled containers ~~where ambient temperature was controlled within 24 ± 2 °C with~~, and a particle pre-impactor ~~to~~ was used to remove particles larger than 10 ~~μm~~μm from the input air stream. The drying systems in the three sites were configured with a Nafion dryer to keep the relative humidity of sample flow below 40%. This type of dryer performs ~~good~~ well in reducing aerosol losses. The transmission efficiency of the Nafion dryer is up to 90% for particles smaller than 10 nm and rises up to 100% for particles larger than 30 nm (The performance details of the Nafion dryer can be accessed at http://www.permapure.com).

During the field campaign at the Zhangqiu site, the particle number size distribution (PNSD) as well as BCPMSD were simultaneously determined using the measurement system developed by Ning et al. (2013)~~. The instrument setup was further~~ and improved by Zhao et al. (2019b). The polydisperse aerosol sample flow was first drawn into DMA (Model 3080, TSI, USA) to select relatively monodispersed aerosol sub-populations with diameters ranging from 97 to 602 nm. Sheath and sample flows were set as 3 and 0.5 L/min, respectively. The selected monodispersed aerosol populations were further divided into two paths. One path (0.2 L/min) was drawn into AE51 for ~~m_{BC}~~ EBC measurements. The other path (0.3 L/min) was analyzed using CPC (model 3772, TSI, USA) for number concentration measurements. As the standard sample flow for CPC 3772 is 1 L/min, a cleaned airflow of 0.7 L/min was added for compensation. A BCPMSD cycle measured here required 5 min and we averaged the data with a temporal resolution of 2 hours.

The dry aerosol scattering coefficients at 525 nm were measured simultaneously to represent air pollution condition by an integrated nephelometer (Ecotech Pty Ltd., Aurora 3000) with ~~a~~ flow ~~r~~rate of 3 L/min~~.~~ and ~~The~~ temporal resolution ~~was~~ of 1 min. Similar to the measured BCPMSD, aerosol scattering coefficients ~~that were used to represent air pollution conditions~~ were also averaged with a temporal resolution of 2 hours.

~~While observing BCPMSD at the Beijing site, added AE33 (3 L/min) simultaneously to measure the bulk m_{BC}. The bulk m_{BC} from AE33 and from the integrated BCPMSD measured by AE51 were then compared.~~ For AE51, the influence of loading effect was resolved by using $\sigma_{ab,corrected} = (1 + k \cdot ATN)\sigma_{ab,uncorrected}$. $\sigma_{ab,corrected}$ and $\sigma_{ab,uncorrected}$ are the corrected and uncorrected

带格式的: 字体: 加粗

带格式的: 字体: 10 磅

σ_{ab}, respectively. Factor k ~~was~~ is set as 0.004 (Zhao et al., 2019b) and ATN is the measured light attenuation ~~when~~ by particles ~~load~~ collected on the ~~fiber~~ filter of AE51. A recommended compensation of 2.6 for AE51 ~~was~~ is introduced here to mitigate the multiple scattering problem (Zhang et al., 2018). Zhao et al. (2019b) added AE33 (3 L/min) to measure the bulk EBC simultaneously while measuring BCPMSD. The bulk EBC from AE33 and the integrated EBC from BCPMSD measured by AE51 were then compared. Results showed that the variation trends and magnitudes of ~~m_{BC}~~ EBC measured by AE33 and AE51 were in good consistence~~.~~. Therefore, ~~in this study,~~ the BCPMSD measured by AE51 was regarded as the measurement results of AE33, and the size-resolved σ_{ab} were retrieved by the constant MAC value of 7.77 m^2/g used in AE33. The traditional BCPMSD is retrieved from AE51-measured size-resolved σ_{ab} with a constant MAC value of 7.77 m^2/g used for AE33. In our new method, the MAC is variable as a function of BC core size (D_{BC}) and particle diameter ($D_{particle}$).

~~For the coupling DMA-SP2 system measurement, the dried sample flow was drawn into DMA to select particles with diameters ranging from 200 to 450 nm. Then, the selected monodispersed aerosol samples were analyzed in SP2 (0.12 L/min) to identify the BC-containing particles and in CPC (0.28 L/min) to count the total number of particles. The size-resolved number fraction of BC-containing particles was then derived. As the total flowrate was 0.4 L/min from DMA, the sheath flow of DMA was 4 L/min. Detailed configuration of the DMA-SP2 system has been demonstrated in a previous study . According to the measurements from Taizhou, only 17% of the ambient particles that contained BC averagely for bulk aerosol populations.~~

For scattering correction, a scattering correction factor C_f is required to account for the scattering effect of the filter matrix: $\sigma_{ab,corrected} = \sigma_{ab,uncorrected}/C_f$. C_f is determined by simultaneous measurement of σ_{ab} by PASS-3 ($\sigma_{ab,PASS-3}$) and AE33 ($\sigma_{ab,AE33}$). $\sigma_{ab,PASS-3}$ is considered as $\sigma_{ab,corrected}$ and $\sigma_{ab,AE33}$ is considered as $\sigma_{ab,uncorrected}$. The wavelengths of PASS-3 and AE33 are not the same. ~~We adjusted t~~The measured wavelengths of AE33 (370 nm, 470 nm, 520 nm, 590 nm, 660 nm, 880 nm and 950 nm) were interpolated to the measured wavelengths of PASS-3 (405 nm, 532 nm, and 781 nm). Specifically, For AE33, 405 nm, 532 nm and 781 nm are calculated at wavelengths pairs of (370 nm, 470 nm), (520 nm, 590 nm) and (660 nm, 880 nm) through Ångström relationship:

$$\frac{\sigma_{ab}(\lambda_1)}{\sigma_{ab}(\lambda_2)} = \left(\frac{\lambda_1}{\lambda_2}\right)^{-\alpha_{ab}}.$$

More detailed information can be found in Zhao et al. (2020). Measurement results ~~from~~ at Taizhou and Beijing showed that all the ratios of σ_{ab} measured by AE33 with a measurement flowrate of 3 L/min and PASS-3 with ~~a measurement~~ flowrate of 1 L/min at the three wavelengths varied slightly over the East and North China Plain (± 0.04), with ~~the~~ an average value ~~at~~ of 2.9. Therefore, as the measurement results between AE33 and AE51 were consistent, all the size-resolved σ_{ab} from AE51 adopted in this study were corrected ~~through the mean ratio~~with $C_f = 2.9$ ~~of 2.9~~.

For the SP2 system, the aerosol samples were analyzed in SP2 (0.12 L/min) to identify the BC-containing particles and in CPC (0.28 L/min) to count the total number of particles. When a BC-containing particle travels through the laser beam (1064 nm) inside the SP2, it emits incandescent light. The avalanche photodetectors (APDs) around the laser beam can detect the incandescence signal. Then the BC-containing particle is detected. N_{BC} can be determined as the ratio of the number of BC-containing particle to

带格式的: 下标
带格式的: 下标
带格式的: 字体: 10 磅
带格式的: 字体: 10 磅
带格式的: 字体: 10 磅
带格式的: 字体: 10 磅
带格式的: 字体: 10 磅
带格式的: 字体: 10 磅
带格式的: 字体: 10 磅
带格式的: 字体: 10 磅
带格式的: 字体: 10 磅
带格式的: 字体: 10 磅
带格式的: 字体: 10 磅
带格式的: 字体: 10 磅
带格式的: 字体: 10 磅
带格式的: 字体: 10 磅
带格式的: 字体: 10 磅
带格式的: 字体: 10 磅
带格式的: 字体: 10 磅
带格式的: 下标

that of total aerosol particle. Detailed configuration of the SP2 system has been demonstrated in a previous study (Zhao et al., 2019a). According to the measurements at Taizhou, only 17% of the ambient particles contained BC averagely for bulk aerosol populations. All the measurement systems at the three sites are shown in Fig. S1 in the supplement.

带格式的

3 Method

For current filter-based intruments, ~~m_{BC}~~EBC are generally derived from σ_{ab} under assumption of~~through~~ a constant MAC value. However, the MAC values are enhanced by different degrees when BC particles are mixed with other weakly-absorbing materials, leading to large uncertainties on ~~BC mass~~EBC retrieval ~~and further evaluations of BC atmospheric optical effects~~. In order to gain more accurate ~~atmospheric BC mass loading~~EBC, it is critical to consider the discrepancies in MAC caused by variations in the coating process, BC sizes, etc. Among with the core-shell configuration hypothesis, developing the relationship between MAC, D_{BC}, and T_{shell} is a new approach to correlate ~~m_{BC}~~ EBC with σ_{ab}.

3.1 Core-shell geometry of aerosol particles

To evaluate the theoretical discrepancies in MAC values caused by the corresponding impact factors, ~~an appropriate model simulation is needed for representing a single BC particle's optical properties~~a proper model is required to simulate the optical properties of BC-containing particles to a good approximation. ~~There are three widely employed mixing states that are used to represent the structure of BC-containing aerosols~~Three widely employed mixing states are used to represent the structure of BC-containing aerosols: internal, external, and core-shell model (Ma et al., 2011;China et al., 2015). Generally, newly-emitted BC particles are chain-like aggregates ~~composed~~ of small spheres. During the coating process, the chain-like BC aggregates become more compact as they collapse and are coated as a core by organic and inorganic materials (Bond and Bergstrom, 2006). Therefore, core-shell configuration is more plausible (Jacobson, 2000). Ma et al. (2012) also indicated that the core-shell assumption can provide a better performance in optical closure than the internal or external models. Furthermore, Moffet et al. (2016) studied particle mixing state and morphology using scanning transmission X-ray microscopy and highlighted that core-shell structure dominated the mixing state of ambient aerosol particles. As aerosols are assumed to be core-shell mixed, with a spherical BC core in the center of the coating sphere~~, the spherical core and shell favor the Mie model~~. Therefore, the Mie model was used ~~in this study~~ to simulate the optical properties of BC particles with core-shell mixing state. The consistency in observed and theoretical values obtained using Mie and core-shell morphology support the suitability of this method (Cappa et al., 2012).

3.2 ~~Mie modeled MAC of BC particles~~Simulation of MAC for BC-containing particle using Mie theory

Many optical simulations for BC particles with concentric sphere geometry have been reported and the corresponding results show that the absorption of a pure BC particle will be enhanced when a shell composed of non-absorbing material deposits on this pure BC particle. Since ~~we focused on~~ the optical properties were focused on rather than chemical compositions of the mixed aerosols, a simplified hypothesis of BC/sulfate mixtures, which is ~~frequent~~ common in the atmosphere (Khalizov et al., 2009), was introduced in the algorithm for calculating ~~m_{BC}~~EBC.

The reason of AE33 using 880 nm to determine EBC is that aerosol absorption at 880 nm is mainly from BC (Ramachandran and Rajesh, 2007). At shorter wavelength, absorption of organic carbon is not negligible any more, leading to difficulty of extracting

BC absorption from total aerosol absorption. Therefore, MAC at 880 nm is discussed in this study ~~Since the filter-based instruments (AE33) use σ_{ab} at the wavelength of 880 nm to determine m_{BC},~~and the MAC distribution for a wide range of core and coating sizes at the wavelength of 880 nm~~, calculated using the~~ are simulated with Mie scattering theory~~, has been presented~~. The refractive index (RI), ~~reported to vary with incident light wavelength~~dependent on light wavelength, is an important parameter to determine aerosol optical properties. However, ~~as BC particles can be emitted from different fuels and conditions, RI cannot be observed directly, with both real and imaginary part of RI varying over a significantly wide range~~due to different sources of BC, both the real and imaginary part of RI varies over a significantly wide range. Liu et al. (2018) summarized RI values for specific wavelengths and showed that the real part is generally in the range of 1.5 to 2.0 while the imaginary part usually varies from 0.5 to 1.1 (Sorensen, 2001;Bond and Bergstrom, 2006). Therefore, the real part and imaginary part of RI were set to change from 1.5 to 2.0 and from 0.5 to 1.1, respectively, with a step increase of 0.01. Meanwhile, the RI of sulfate was set as 1.55-1.0^{-6} i and the density of BC was set as 1.8 g/cm^3, similar to Bond et al. (2006). A total of 3111 values were obtained, and the ~~averaged~~ mean values are illustrated in Fig. 1. The D_{BC} and total aerosol particle diameter ($D_{particle}$, D_{BC} + T_{shell}) ranged from 10 to 700 nm.

Figure 1 presents several features of the variation pattern of MAC at 880 nm. MAC values varied significantly with D_{BC} and the thickness of non-absorbing coating, which indicated that light absorption of BC-containing particles was sensitive to the BC core and the coating. When the D_{BC} was less than 100 nm, the thickness of the coating dominated the variation of MAC values, and MAC values increased with increasing T_{shell}. As the ~~value~~ T_{shell} increased, the lensing effect became more significant, the light absorption consequently also increased with increasing T_{shell}. MAC value can increase from 4 m^2/g to about 17 m^2/g when the total aerosol size reached up to 700 nm, which indicated that light absorption can be enhanced significantly by the coating. When the D_{BC} was larger than about 100 nm, both T_{shell} and D_{BC} determined MAC values and D_{BC} played a more important role considering that the majority of the contour lines tilted to the axis of particle diameter. MAC increased with increasing T_{shell} and decreased with ~~the~~ increasing D_{BC}. At this range (D_{BC} > 100 nm), the coating still enhanced absorption. –For pure BC particle, MAC decreased with increasing D_{BC} when D_{BC} > ~ 220 nm, which indicated that the absorption of large BC particles was less than that of small BC particles per unit mass. If the $D_{particle}$ or the coating (T_{shell}) was fixed, larger D_{BC} generally corresponded to a smaller MAC. Not only did the MAC of coated BC-containing particle vary significantly, but the variation of MAC of pure BC particle was also nonnegligible. ~~Moreover, even for pure BC particles, MAC values varied significantly with the size of BC particles.~~ For smaller pure BC particle~~s~~, the MAC ~~values~~ increased slightly with BC size until D_{BC} reached 220 nm. Then, MAC decreased with ~~an increase increasing~~~~in~~ D_{BC}. Therefore, light absorption can be significantly influenced by coating state, and ~~the~~ a constant MAC value of 7.77 m^2/g used in AE33 is only appropriate for a very limited condition.

3.3 New method to retrieve ~~m_{BC}~~EBC by considering the variation of MAC

In this subsection, ~~we introduce~~ a new method is introduced to determine ~~m_{BC}~~ EBC from the measure~~ment of the~~d σ_{ab} ~~at a given diameter~~. ~~For~~ At a given $D_{particle}$ (=D_{BC} + T_{shell}) selected by DMA, if D_{BC} is prescribed~~assumed~~, the corresponding T_{shell} is determined~~is fixed~~. Combining the simultaneously measured ~~PNSD~~particle number concentration ($N(D_{particle})$) by CPC downstream the DMA and the prescribed ~~percentage of particles containing BC~~N_{BC}, the number of BC-containing particles ($N_{BC}(D_{particle})$) is then

带格式的: 下标
带格式的: 下标
带格式的: 下标
带格式的: 下标
带格式的: 下标
带格式的: 非上标/ 下标
带格式的: 非上标/ 下标
带格式的: 下标
带格式的: 下标
带格式的: 下标
带格式的: 下标

determined ~~at $D_{particle}$~~. σ_{ab} can then be calculated by Mie model with $D_{particle}$, D_{BC} and $N_{BC}(D_{particle})$.~~Corresponding absorption properties at the $D_{particle}$ with fixed D_{BC} and T_{shell} can be calculated using the Mie model.~~ If the calculated σ_{ab} matches measured σ_{ab} by AE51, then the prescribed D_{BC} is considered as diameter of BC core at $D_{particle}$. Else, D_{BC} is changed until calculated σ_{ab} equals measured σ_{ab}. MAC can be calculated by Mie model with $D_{particle}$, D_{BC} and a presumed BC density. EBC at $D_{particle}$ is then derived by dividing measured σ_{ab} by MAC. BCPMSD can then be derived through changing $D_{particle}$ selected by DMA.~~Hence, if the number concentration of BC-containing particles and σ_{ab} at a given $D_{particle}$ are measured, we can infer the D_{BC} by closing the measured and the calculated σ_{ab}. Then, the m_{BC} can be obtained from D_{BC} for every $D_{particle}$. Finally, the BCPMSD is derived.~~

~~The detailed iterative procedure is illustrated in Fig. 2.~~ As the absorption properties of BC particles in different coating states have been evaluated with the Mie model, as ~~represented~~ shown in Fig. 1, a simplified algorithm was proposed for deriving BCPMSD ~~was proposed by considering Fig. 1 as a~~ through a pre-calculated look-up table. For ~~every specific~~each $D_{particle}$ selected by DMA, if a D_{BC} is assumed, the corresponding MAC of the particle can be derived from the look-up table. Then, the σ_{ab} can be derived from the MAC, the assumed BC density (1.8 g/cm^3 in this study), and ~~the number of BC-containing particles~~N_{BC} (17% ~~of the total number~~ for ~~every~~ each $D_{particle}$). We adjusted the guessed D_{BC} until the difference between calculated and measured σ_{ab} was within an acceptable range (0.1%). Consequently, the D_{BC} and thus the ~~m_{BC}~~ EBC at ~~a given~~ $D_{particle}$ was determined. The ~~m_{BC}~~ EBC at different aerosol sizes were derived separately. Finally, the size-resolved ~~m_{BC}~~ EBC and the bulk ~~m_{BC}~~ EBC were obtained. The ~~detailed~~ iterative procedure is illustrated in Fig. 2.

It should be pointed out that the retrieval algorithm of BCPMSD is based on the assumption that BC-containing particles of a fixed diameter are all core-shell mixed and the corresponding D_{BC} for a specific $D_{particle}$ is same. The uncertainties caused by idealized core-shell model was discussed in section 5.1. ~~Moreover, a~~A constant number percentage (17%) of BC-containing particles was adopted in this study. However, the BC-containing particle fraction varied with the primary source, time, coagulation, and extent of atmospheric process. The influence attributed to the constant fraction of BC-containing particles ~~has been~~was discussed in section ~~2 of the supplement~~5.2. Additionally, Bond et al. (2013) summarized the density for different graphitic materials. The density values are 1.8 – 2.1 g/cm^3 for pure graphite, 1.8 – 1.9 g/cm^3 for pressed pellets of BC, and 1.718 g/cm^3 for fullerene soot. A constant density (1.8 g/cm^3) for BC was briefly used to calculate MAC and BC mass from the volume of particles with a diameter of D_{BC}. Therefore, the uncertainty of derived ~~m_{BC}~~ EBC in this study simply depends on the ratio of 1.8 g/cm^3 and the real density. Finally, the MAC values in the look-up table were the ~~averaged~~ mean values for different RI and the corresponding effects ~~have been~~were discussed in section 5.3.

4 Results and discussion

Figure 3 provides a comprehensive overview of the variations in measured and retrieved size-resolved parameters during the campaign. As evident from Fig. 3(a), for the BCPMSD derived by the new method, two modes were found~~, similar to the results of AE33~~. Figure 4(a) shows the averaged BCPMSD derived from the new method and AE33 during the campaign. The ~~finer~~fine mode was located between 97 – 240 nm while the ~~coarser~~coarse mode was located between 240 – 602 nm. Figure 3(b) represents the relative deviations between the BCPMSD derived from the new proposed method and those derived from a constant MAC value of

带格式的: 下标
带格式的: 下标
带格式的: 下标
带格式的: 下标
带格式的: 下标
带格式的: 非上标/ 下标
带格式的: 下标

7.77 m^2/g at 880 nm. The results show that there exist two opposite deviation trends before and after the turning point around 280nm.~~The results indicate that with the boundary of 280 nm, two opposite deviation tendencies exist.~~ For aerosol particles larger than 280 nm, the ~~m_{BC}~~ EBC derived by the new method were mostly lower than those derived with the constant MAC value of 7.77 m^2/g at 880 nm. In contrast, when aerosol particles were smaller than 280 nm, the ~~m_{BC}~~ EBC from the new method were significantly higher than those calculated by the constant MAC, as shown in Fig. 3(c). Figure 3(c) shows the time series of size-resolved MAC during the derivation process of BCPMSD. According to Fig. 3(c), for aerosol particles smaller than 280 nm, the corresponding MAC was almost lower than 7.77 m^2/g at 880 nm. This is because the MAC values of particles smaller than 280 nm are mostly lower than 7.77 m^2/g, as represented in Fig. 1. A smaller MAC implies a weaker absorption ability, which means that the same measured σ_{ab} will correspond to an increased ~~m_{BC}~~EBC. Therefore, more ~~BC mass loadings~~EBC were derived from the new method. For aerosol particles larger than 280 nm, in order to match the measured σ_{ab}, the corresponding D_{BC} were generally found to be in those regions of look-up table where the MAC values were larger than 7.77 m^2/g at 880 nm ~~–~~(Fig. 3(c)). Thus, the BC mass loadings for particles larger than 280 nm were found to be less than those calculated with the constant MAC value of 7.77 m^2/g at 880 nm. From Fig. 3(c), it can be seen that MAC varied from less than 4 m^2/g to larger than 10 m^2/g at 880 nm, which implies a large variability of the absorption ability of BC-containing particle. Therefore, if the conversion between m_{BC} and σ_{ab} is required, the consideration of variation in mixing state is highly recommended. The simultaneously measured scattering coefficients at 525 nm were introduced here to represent air pollution. As shown in Fig. 3(d), the observation station experienced different levels of pollution. Deviations of ~~m_{BC}~~ EBC derived from the newly proposed method and the constant MAC at different aerosol sizes did not show dependencies on pollution conditions.

Figure 3(e) shows the time series of ~~m_{BC}~~ EBC at ~~finer~~fine and ~~coarser~~coarse modes. ~~Compared to the results of AE33, t~~The ~~m_{BC}~~ EBC were more concentrated in the ~~finer~~fine mode ~~as compared to~~than in the ~~coarser~~coarse mode. The ~~m_{BC}~~ EBC at ~~finer~~fine mode were found to be higher than those at the ~~coarser~~coarse mode for 73% of the ~~experiment~~ campaign duration. The variation trends of bulk ~~m_{BC}~~ EBC calculated by considering the variations of MAC and a constant MAC were similar (Fig. 3(f)). The bulk ~~m_{BC}~~ EBC calculated by the new method were higher than those derived by the constant MAC in 83% of the ~~experiment~~ campaign duration.

The ~~m_{BC}~~ EBC calculated from the new method and AE33 for different aerosol size ranges were statistically analyzed. As shown in Fig. 4, for all ~~m_{BC}~~ EBC of aerosols ranging between 97 – 602 nm and 97 – 280 nm derived from new method and AE33, strong linear relationships were observed with correlation coefficients of 0.99 and 1.00, respectively. The ratios between the ~~m_{BC}~~ EBC derived from AE33 and the new method for aerosol diameter ranges of 97 – 602 nm and 97 – 280 nm were 0.84 and 0.69, respectively, indicating that the ~~m_{BC}~~ EBC obtained from AE33 was 16% lower for bulk aerosol particles and 31% lower for aerosols smaller than 280 nm. For the diameter range of 280 – 602 nm, MAC values varied significantly and the deviations in ~~m_{BC}~~ EBC derived from the new method and AE33 were divided into two types with a boundary of 0.7 $\mu g/m^3$. If the ~~m_{BC}~~ EBC derived from AE33 was lower than 0.7 $\mu g/m^3$, there was a relatively consistent ratio of 1.13 between the ~~m_{BC}~~ EBC from the new method and AE33, with a correlation coefficient of 0.95. Therefore, BC mass loading from the AE33 algorithm was 13% higher for aerosol particles larger than 280 nm and ~~m_{BC}~~ EBC lower than 0.7 $\mu g/m^3$. However, when the ~~m_{BC}~~ EBC derived from AE33 was larger than 0.7 $\mu g/m^3$, data

带格式的: 上标
带格式的: 上标
带格式的: 下标

points become discrete, and the relationship between the ~~m_{BC}~~ EBC derived from AE33 and the new method could be expressed through an equation (y = 0.29 + 0.48x). However, these comparisons for aerosols at different size ranges were obtained based on the measurements in the NCP. Additionally, the number of samples where ~~m_{BC}~~ EBC of 280 – 602 nm were larger than 0.7 μg/m^3 was too small. Further studies on BCPMSD in conjunction with the PNSD measurements at different sites need to be carried out.

5 Uncertainty analysis

带格式的: 字体: 加粗

5.1 The uncertainties of MAC caused by using idealized core-shell model

An idealized concentric core-shell model with a spherical BC core fully coated by sulfate was configured to study the MAC of BC aerosols and derive the EBC in this study. However, freshly emitted BC particles were found to normally exist in the form of loose cluster-like aggregates with numerous spherical primary monomers (Liu et al., 2015). Soon after, these aggregates become coated with other components and collapsed to a more compact form during the coating process (Zhang et al., 2008;Peng et al., 2016). Therefore, the uncertainty in the idealized core-shell configuration is discussed in this subsection.

5.1.1 The formation of BC aggregates with a determined morphology

The fractal aggregates of BC have been well described by fractal geometries through the well-known statistical scaling law (Sorensen, 2001):

$$N = k_f \left(\frac{R_g}{a}\right)^{D_f},$$

where N is the number of "same-sized" monomers in the cluster, a is the monomer radius, D_f and k_f are known as the fractal dimension and fractal prefactor respectively, determining the morphology of BC cluster. The compactness of a fractal aggregate increses with increasing D_f or k_f. R_g is the gyration radius, infering the overall aggregate radius, determined by

$$\mathrm{R}_g = \sqrt{\frac{1}{N}\sum_{i=1}^{N} r_i{}^2},$$

where r_i represents the distance of the i-th monomer from the center of mass of BC cluster.

In order to generate fractal-like aggregates with given N, R_g, a, D_f and k_f, the sequential algorithm proposed in Filippov et al. (2000) is introduced in this study to add the primary monomers one by one. On condition that there is an aggregate including $N-1$ monomers, the N-th monomer is constantly placed randomly until it has at least one contact point with the previously attached $N-1$ monomers with no overlapping. Besides, the mass center of the next Nth monomer must obey the rule as follows:

$$(r_N - r_{N-1})^2 = \frac{N^2a^2}{N-1}\left(\frac{N}{k_f}\right)^{2/D_f} - \frac{Na^2}{N-1} - Na^2\left(\frac{N-1}{k_f}\right)^{2/D_f},$$

where r_{N-1} and r_N are the mass center of the first $N-1$ monomers and the N-th monomer, respectively. After the fractual configuration of BC aggregates, the absorption properties of BC containing particles need to be evaluated.

The fractal dimensions for aged BC aggregates are generally close to 3 (Kahnert et al., 2012). The aim of this study is to evaluate the effects of aerosol microphysics on the absorption enhancement of fully coated BC particles, which can be regarded as the aged BC aerosols. Therefore, the fractal dimension D_f is set to be 2.8 and k_f is generally set to be 1.2. The diameter of the primary monomers is usually between 20-50 nm and the number of the primary monomers for an aggregates is between 50-300. The size of

BC core calcuated by the new method is smaller than 300 nm most of the time during Zhangqiu campaign. The diameter of primary monomers is set to be 50 nm and the number of the primary monomers for an aggregates ranges from 2 to 200, leading to the largest size of volume equivalent BC core close to 300 nm. The real part of BC is generally in the range of 1.5 to 2.0 while the imaginary part usually varies from 0.5 to 1.1 (Liu et al., 2018). Therefore, the mean value 1.75 for BC real part and 0.8 for BC imaginary part are adopted here to calculate MAC values for BC/sulfate mixtures at the wavelength of 880 nm.

5.1.2 Multiple Sphere T-matrix (MSTM) method

As the traditional Mie model is not available for the fractal aggregates, the widely used MSTM method is employed here to quantify the absorption properties of BC clusters (Mackowski and Mishchenko, 1996;Mackowski, 2014). The addition theorem of vector spherical wave functions is used in MSTM method to describe the mutual interactions among the system. The T-matrix of aggregates used to derive particle optical properties can be obtained from these individual monomers. MSTM method can calculate light scattering and absorption properties of the randomly oriented aggregates without numerical averaging over particle orientations if the position, size and refractive index of every spherical element are given. However, the MSTM method is only applicable to evaluate the aggregates of spheres without overlapping and it is carried out with high computational demand.

The deviations showed in Fig. 5 are derived by subtracting MAC values calculated by MSTM model by those calculated by Mie model. The results show that most of the MAC values calculated by assuming BC particles in the form of cluster-like aggregates are smaller when the size of BC core is smaller than 150 nm and the overall deviation is within 4 %, which indicates that Mie theory is a good approximation to the BC aggregates even when D_{BC} reaches 200 nm. When BC core is larger than 200 nm, the MAC values calculated by MSTM model increase with the thickness of shell and will be larger than those derived from concentric core-shell model. The deviations between MAC calculated by the idealized concentric core-shell model and letting BC particles be in the form of cluster-like aggregates are overall within 15%.

5.2 The uncertainties of derived EBC caused by using a constant BC-containing particle fraction

Figure 6 shows the deviation of BCPMSD calculated from different N_{BC} (8.5%, 17%, 34%). We can see that for our newly proposed method, using a constant N_{BC} does not change the size-resolved distribution mode. There is still a fine mode and coarse mode with a boundary of 240 nm. Besides, the influence of using different N_{BC} to derived EBC is very limited when particles are larger than 200 nm. However, the deviations between the EBC derived from different N_{BC} are large when particles diameters are smaller than 200 nm. At this range, if N_{BC} is underestimated, the EBC will be underestimated. On the contrary, the EBC is overeatimated if N_{BC} is overestimated.

~~5~~ **5.3 The uncertainties of MAC caused by variation of RI~~Influences of RI on MAC~~**

As the RI of BC is still reported to vary over a wide range and the MAC used in this study was a mean value, it is critical to assess the impact caused by variation in the real and imaginary parts of RI on the calculated MAC and the derived ~~BC mass concentrations~~EBC. For aerosol particles with ~~fixed~~ given D_{BC} and T_{shell}, we calculated the MAC of BC with the real part of RI ranging from 1.5 to 2.0 and imaginary part ranging from 0.5 to 1.1. The step increase of both real and imaginary parts was 0.01 and there were 3111 MAC values for every aerosol particle with ~~fixed~~ given D_{BC} ~~core size~~ and T_{shell}. The ratio of the standard deviation

带格式的: 下标

带格式的: 字体: (中文) +中文正文 (等线), (中文) 中文(中国)

带格式的: 字体: 10 磅

带格式的: 字体: 10 磅

带格式的: 定义网格后自动调整右缩进, 调整中文与西文文字的间距, 调整中文与数字的间距

带格式的: 字体: (中文) 等线, 非加粗, 不检查拼写或语法

带格式的: 下标

to the mean value for these 3111 MAC values have been presented to demonstrate the uncertainty in MAC due to the uncertainty of BC RI.~~–~~

Figure ~~5~~7(a) shows the uncertainties in MAC along different values of D_{BC} and T_{shell}. It shows that aerosol particles with ~~a~~ small BC core have larger uncertainties and all the uncertainties were below 24%, implying a large variation in absorption for BC-containing particle with small BC core. When $D_{particle}$ was fixed, the uncertainties decreased with increasing D_{BC}. When D_{BC} was determined, the uncertainties did not change much with T_{shell}~~:~~, indicating the importance to quantify D_{BC} for BC-containing particles in order to reduce RI-related uncertainty in absorption. For pure BC particles, the uncertainties also decreased with increasing BC particle size significantly from over 22% at 100 nm to less than 2% at 600 nm. Figure ~~5~~7(b) shows the uncertainties when the imaginary part was fixed at 0.8 and the real part ranged from 1.5 to 2.0 with an interval of 0.01. It can be seen that when the imaginary part of RI was fixed, variations in the real part led to slight uncertainties. All the uncertainties were found to be below 14%. Figure ~~5~~7(c) demonstrates the uncertainties when the real part was fixed at 1.75 and the imaginary part ranged from 0.5 to 1.1 with an interval of 0.01. Comparing Fig. ~~5~~7(a) and ~~5~~7(c), we can see that the patterns of MAC uncertainties were similar. Overall, the uncertainties were dominated by the variations of the imaginary part and only slightly affected by variations in the real part. Therefore, it is highly recommended to reduce the uncertainties in the imaginary part for a more precise absorption measurement.

The variation~~s~~ ~~in~~ of ~~on~~ m_{BC} EBC caused by the uncertainties in RI were further evaluated. As stated in section 3.2, ~~all~~for a MAC (880 nm) point at ~~MACs~~ ($D_{particle}$, D_{BC}) of Fig. 1, it is a mean value averaged with respect to both real part of RI varied from 1.5 to 2.0 and imaginary part of RI varied from 0.5 to 1.1. ~~in the look-up table in Fig. 1 are the mean values as the imaginary part and real part of BC RI varied over a wide range. Therefore, t~~The mean MAC~~s~~ (880 nm) ~~in the look-up table~~ plus corresponding standard deviation (MAC + Std) and minus corresponding standard deviation (MAC – Std) were ~~utilized~~ used to show the uncertainties in ~~m_{BC}~~ EBC caused by variation of BC RI ~~of BC~~. As we can see from Fig. ~~6~~8(a), irrespective of the MAC ~~values in look-up table were~~ was MAC + Std or MAC – Std, there was no change in the mode of BCPMSD. The derived ~~m_{BC}~~ EBC of all ~~aerosols~~ particles ranging from 97 – 602 nm increased when ~~the MAC values used in the look-up table were~~ MAC – Std was used and decreased when MAC + Std ~~values were~~ was used ~~in the look-up table~~. Compared to the bulk ~~m_{BC}~~ EBC ~~retrieved~~ derived ~~through the look-up table with~~by mean MAC, those derived ~~through the look-up table with~~by MAC – Std were higher within 35% (Fig. ~~6~~8(b)). The decrease in the ~~magnitude of~~ derived ~~m_{BC}~~ EBC caused by MAC + Std ~~values~~ was ~~significantly~~ less than the increase in the ~~magnitude~~derived EBC caused by the MAC – Std ~~values~~. ~~Similarly, f~~For ~~aerosol particles at~~ both ~~finer~~fine and ~~coarser~~coarse ~~modes~~mode particles, the deviations in ~~m_{BC}~~ EBC caused by MAC + Std or MAC – Std were also within 35% (Fig. ~~6~~ 8(c) and Fig. ~~6~~ 8(d)). ~~Meanwhile, the increase in the magnitude of derived σ_{ab} into m_{BC} caused by the MAC-Std values was also significantly higher than the decrease in the magnitude caused by the MAC + Std values.~~ This sensitivity study ~~indicated~~ indicates that the accuracy of the ~~retrieved~~ derived BCPMSD is sensitive to the accuracy of MAC ~~values in the look-up table~~, especially when the ~~real~~ actual MAC~~s~~ ~~are~~ is less than the mean MAC ~~values used in the look-up table~~.

~~An idealized concentric core-shell model with a spherical BC core fully coated by sulfate was configured to study the MAC of BC aerosols and derive the m_{BC}. However, freshly emitted BC particles were found to normally exist in the form of loose cluster-like~~

带格式的: 下标

带格式的: 下标

带格式的: 下标

带格式的: 非上标/ 下标

~~aggregates with numerous spherical primary monomers . Soon after, these aggregates become coated with other components and collapsed to a more compact form during the coating process . Therefore, the uncertainty in the idealized core-shell configuration is discussed in section 3 of the supplement.~~

6 Conclusions

There was a significant variability in the MAC values of BC with the size of BC core and the thickness of coating, which exerted a significant influence on the optical method for ~~measuring m_{BC}~~deriving EBC. In this study, a new method was proposed to derive ~~m_{BC}~~ EBC~~while~~ considering the lensing effect of core-shell structure and ~~subsequently~~ the consequent MAC variations in MAC~~of BC~~.

A look-up table describing the variations of MAC at 880 nm attributed to the coating state and size of BC core was established theoretically using Mie simulation and assuming a core-shell configuration for BC-containing aerosols. The MAC at 880 nm varied significantly with different sizes of core and shell from less than 2 m^2/g to over 16 m^2/g, indicating a large variation in absorption ability for BC-containing particle. Then, the ~~m_{BC}~~ EBC at different aerosol sizes were derived by finding an appropriate BC core configured with a MAC value from the look-up table to close the calculated and measured σ_{ab}.

This newly proposed method was applied to a campaign measurement in the NCP. There were two modes for BCPMSD at the accumulation mode separated by 240 nm. For 73% of the cases, the ~~m_{BC}~~ EBC of the ~~finer~~fine mode were larger than those of the ~~coarser~~coarse mode during the measurement. The ~~m_{BC}~~ EBC derived by the new method were mostly lower than those derived by a constant MAC of 7.77 m^2/g for particles larger than 280 nm, and higher for particles smaller than 280 nm. Similarly, the bulk ~~m_{BC}~~ EBC accumulated from BCPMSD derived from the new method were mostly higher than those derived from a constant MAC of 7.77 m^2/g.

Uncertainty analysis was carried out with respect to assumptions used in this study. The uncertainty caused by idealized core-shell model was analyzed by substituting the core with cluster-like aggregates using MSTM method, and the resulting relative uncertainties were within 15%. The uncertainties caused by using a constant number fraction of BC-containing particle was analyzed by halving and doubling its value, and the results showed that particle larger than 200 nm was insensitive to the number fraction of BC-containing particle, whereas, for particle smaller than 200 nm, the EBC would be underestimated if the BC-containing particle fraction was underestimated. The uncertainty in derived ~~m_{BC}~~ EBC that was caused due to the wide range of RI of the BC core was also studied. The results indicated that the uncertainty of the imaginary part results in larger uncertainties to the MAC ~~as~~ compared ~~to~~ with the real part. The relative uncertainty of the derived ~~m_{BC}~~ EBC was within 35%.

This study provides a new way to derive ~~m_{BC}~~ EBC from σ_{ab} for the widely-used filter-based measurements. This research deepens our understanding of the uncertainty in measured ~~m_{BC}~~ EBC caused by the utilization of a constant MAC and illustrates the great necessity to take the variation of MAC into account. The new method improves the measurements of BCPMSD and ~~is further beneficial to the evaluation of BC radiative forcing~~deepens the understanding about the significant influence of mixing state on the absorption of BC.

Data availability

带格式的: 上标

带格式的: 上标

The measurement data involved in this study are available upon request to the authors.

Author contributions

CZ determined the main goal of this study. WZ and WT designed the methods. WZ carried them out and prepared the paper with contributions from all co-authors.

Competing interests

The authors declare that they have no conflict of interest.

References

Adler, G., Riziq, A. A., Erlick, C., and Rudich, Y.: Effect of intrinsic organic carbon on the optical properties of fresh diesel soot, Proceedings of the National Academy of Sciences of the United States of America, 107, 6699-6704, 10.1073/pnas.0903311106, 2010.

Arnott, W. P., Hamasha, K., Moosmuller, H., Sheridan, P. J., and Ogren, J. A.: Towards aerosol light-absorption measurements with a 7-wavelength Aethalometer: Evaluation with a photoacoustic instrument and 3-wavelength nephelometer, Aerosol Science and Technology, 39, 17-29, 10.1080/027868290901972, 2005.

Bond, T. C., Anderson, T. L., and Campbell, D.: Calibration and intercomparison of filter-based measurements of visible light absorption by aerosols, Aerosol Science and Technology, 30, 582-600, 10.1080/027868299304435, 1999.

Bond, T. C., and Bergstrom, R. W.: Light absorption by carbonaceous particles: An investigative review, Aerosol Science and Technology, 40, 27-67, 10.1080/02786820500421521, 2006.

Bond, T. C., Habib, G., and Bergstrom, R. W.: Limitations in the enhancement of visible light absorption due to mixing state, J. Geophys. Res.-Atmos., 111, 13, 10.1029/2006jd007315, 2006.

Bond, T. C., Doherty, S. J., Fahey, D. W., Forster, P. M., Berntsen, T., DeAngelo, B. J., Flanner, M. G., Ghan, S., Karcher, B., Koch, D., Kinne, S., Kondo, Y., Quinn, P. K., Sarofim, M. C., Schultz, M. G., Schulz, M., Venkataraman, C., Zhang, H., Zhang, S., Bellouin, N., Guttikunda, S. K., Hopke, P. K., Jacobson, M. Z., Kaiser, J. W., Klimont, Z., Lohmann, U., Schwarz, J. P., Shindell, D., Storelvmo, T., Warren, S. G., and Zender, C. S.: Bounding the role of black carbon in the climate system: A scientific assessment, J. Geophys. Res.-Atmos., 118, 5380-5552, 10.1002/jgrd.50171, 2013.

Boucher, O., D. Randall, P. Artaxo, C. Bretherton, G. Feingold, P. Forster, V.-M. Kerminen, Y. Kondo, H. Liao, U. Lohmann, P. Rasch, S.K. Satheesh, S. Sherwood, B. Stevens, and Zhang, X. Y.: Clouds and Aerosols. In: Climate Change 2013: The Physical Science Basis. Contribution of Working Group I to the Fifth Assessment Report of the Intergovernmental Panel on Climate Change, in, edited by: Stocker, T. F., D. Qin, G.-K. Plattner, M. Tignor, S.K. Allen, J. Boschung, A. Nauels, Y. Xia, V. Bex and P.M. Midgley, Cambridge University Press, Cambridge, United Kingdom and New York, NY, USA, 571-657, 2013.

Brem, B. T., Gonzalez, F. C. M., Meyers, S. R., Bond, T. C., and Rood, M. J.: Laboratory-Measured Optical Properties of Inorganic and Organic Aerosols at Relative Humidities up to 95%, Aerosol Science and Technology, 46, 178-190, 10.1080/02786826.2011.617794, 2012.

Cappa, C. D., Onasch, T. B., Massoli, P., Worsnop, D. R., Bates, T. S., Cross, E. S., Davidovits, P., Hakala, J., Hayden, K. L., Jobson,

带格式的: 字体: 10 磅

B. T., Kolesar, K. R., Lack, D. A., Lerner, B. M., Li, S. M., Mellon, D., Nuaaman, I., Olfert, J. S., Petaja, T., Quinn, P. K., Song, C., Subramanian, R., Williams, E. J., and Zaveri, R. A.: Radiative Absorption Enhancements Due to the Mixing State of Atmospheric Black Carbon, Science, 337, 1078-1081, 10.1126/science.1223447, 2012.

Cappa, C. D., Zhang, X. L., Russell, L. M., Collier, S., Lee, A. K. Y., Chen, C. L., Betha, R., Chen, S. J., Liu, J., Price, D. J., Sanchez, K. J., McMeeking, G. R., Williams, L. R., Onasch, T. B., Worsnop, D. R., Abbatt, J., and Zhang, Q.: Light absorption by ambient black and brown carbon and its dependence on black carbon coating state for two California, USA, cities in winter and summer, J. Geophys. Res.-Atmos., 124, 1550-1577, 10.1029/2018jd029501, 2019.

Castagna, J., Calvello, M., Esposito, F., and Pavese, G.: Analysis of equivalent black carbon multi-year data at an oil pre-treatment plant: Integration with satellite data to identify black carbon transboundary sources, Remote Sens. Environ., 235, 10, 10.1016/j.rse.2019.111429, 2019.

China, S., Scarnato, B., Owen, R. C., Zhang, B., Ampadu, M. T., Kumar, S., Dzepina, K., Dziobak, M. P., Fialho, P., Perlinger, J. A., Hueber, J., Helmig, D., Mazzoleni, L. R., and Mazzoleni, C.: Morphology and mixing state of aged soot particles at a remote marine free troposphere site: Implications for optical properties, Geophys. Res. Lett., 42, 1243-1250, 10.1002/2014gl062404, 2015.

Chung, C. E., Ramanathan, V., and Decremer, D.: Observationally constrained estimates of carbonaceous aerosol radiative forcing, Proceedings of the National Academy of Sciences of the United States of America, 109, 11624-11629, 10.1073/pnas.1203707109, 2012.

Doran, J. C., Barnard, J. C., Arnott, W. P., Cary, R., Coulter, R., Fast, J. D., Kassianov, E. I., Kleinman, L., Laulainen, N. S., Martin, T., Paredes-Miranda, G., Pekour, M. S., Shaw, W. J., Smith, D. F., Springston, S. R., and Yu, X. Y.: The T1-T2 study: evolution of aerosol properties downwind of Mexico City, Atmospheric Chemistry and Physics, 7, 1585-1598, 10.5194/acp-7-1585-2007, 2007.

Filippov, A. V., Zurita, M., and Rosner, D. E.: Fractal-like aggregates: Relation between morphology and physical properties, J. Colloid Interface Sci., 229, 261-273, 10.1006/jcis.2000.7027, 2000.

Fuller, K. A., Malm, W. C., and Kreidenweis, S. M.: Effects of mixing on extinction by carbonaceous particles, J. Geophys. Res.-Atmos., 104, 15941-15954, 10.1029/1998jd100069, 1999.

Gunter, R. L., Hansen, A. D. A., Boatman, J. F., Bodhaine, B. A., Schnell, R. C., and Garvey, D. M.: Airborne measurement of aerosol optical-properties over south-central New-Mexico, Atmospheric Environment Part a-General Topics, 27, 1363-1368, 10.1016/0960-1686(93)90262-w, 1993.

Hansen, A. D. A., Rosen, H., and Novakov, T.: The aethalometer - an instrument for the real-time measurement of optical-absorption by aerosol-particles, Sci. Total Environ., 36, 191-196, 10.1016/0048-9697(84)90265-1, 1984.

Helin, A., Niemi, J. V., Virkkula, A., Pirjola, L., Teinila, K., Backman, J., Aurela, M., Saarikoski, S., Ronkko, T., Asmi, E., and Timonen, H.: Characteristics and source apportionment of black carbon in the Helsinki metropolitan area, Finland, Atmospheric Environment, 190, 87-98, 10.1016/j.atmosenv.2018.07.022, 2018.

Highwood, E. J., and Kinnersley, R. P.: When smoke gets in our eyes: The multiple impacts of atmospheric black carbon on climate, air quality and health, Environment International, 32, 560-566, 10.1016/j.envint.2005.12.003, 2006.

Jacobson, M. Z.: A physically-based treatment of elemental carbon optics: Implications for global direct forcing of aerosols, Geophys. Res. Lett., 27, 217-220, 10.1029/1999gl010968, 2000.

Jacobson, M. Z.: Strong radiative heating due to the mixing state of black carbon in atmospheric aerosols, Nature, 409, 695-697, 10.1038/35055518, 2001.

Kahnert, M., Nousiainen, T., Lindqvist, H., and Ebert, M.: Optical properties of light absorbing carbon aggregates mixed with sulfate: assessment of different model geometries for climate forcing calculations, Optics Express, 20, 17, 10.1364/oe.20.010042, 2012.

Khalizov, A. F., Xue, H. X., Wang, L., Zheng, J., and Zhang, R. Y.: Enhanced light absorption and scattering by carbon soot aerosol internally mixed with sulfuric acid, Journal of Physical Chemistry A, 113, 1066-1074, 10.1021/jp807531n, 2009.

Lack, D. A., and Cappa, C. D.: Impact of brown and clear carbon on light absorption enhancement, single scatter albedo and absorption wavelength dependence of black carbon, Atmospheric Chemistry and Physics, 10, 4207-4220, 10.5194/acp-10-4207-2010, 2010.

Lack, D. A., Langridge, J. M., Bahreini, R., Cappa, C. D., Middlebrook, A. M., and Schwarz, J. P.: Brown carbon and internal mixing in biomass burning particles, Proceedings of the National Academy of Sciences of the United States of America, 109, 14802-14807, 10.1073/pnas.1206575109, 2012.

Li, Z. J., Tan, H. B., Zheng, J., Liu, L., Qin, Y. M., Wang, N., Li, F., Li, Y. J., Cai, M. F., Ma, Y., and Chan, C. K.: Light absorption properties and potential sources of particulate brown carbon in the Pearl River Delta region of China, Atmospheric Chemistry and Physics, 19, 11669-11685, 10.5194/acp-19-11669-2019, 2019.

Liu, C., Yin, Y., Hu, F. C., Jin, H. C., and Sorensen, C. M.: The effects of monomer size distribution on the radiative properties of black carbon aggregates, Aerosol Science and Technology, 49, 928-940, 10.1080/02786826.2015.1085953, 2015.

Liu, C., Chung, C. E., Yin, Y., and Schnaiter, M.: The absorption Angstrom exponent of black carbon: from numerical aspects, Atmospheric Chemistry and Physics, 18, 6259-6273, 10.5194/acp-18-6259-2018, 2018.

Liu, H., Pan, X. L., Wu, Y., Wang, D. W., Tian, Y., Liu, X. Y., Lei, L., Sun, Y. L., Fu, P. Q., and Wang, Z. F.: Effective densities of soot particles and their relationships with the mixing state at an urban site in the Beijing megacity in the winter of 2018, Atmospheric Chemistry and Physics, 19, 14791-14804, 10.5194/acp-19-14791-2019, 2019.

Ma, N., Zhao, C. S., Nowak, A., Muller, T., Pfeifer, S., Cheng, Y. F., Deng, Z. Z., Liu, P. F., Xu, W. Y., Ran, L., Yan, P., Gobel, T., Hallbauer, E., Mildenberger, K., Henning, S., Yu, J., Chen, L. L., Zhou, X. J., Stratmann, F., and Wiedensohler, A.: Aerosol optical properties in the North China Plain during HaChi campaign: an in-situ optical closure study, Atmospheric Chemistry and Physics, 11, 5959-5973, 10.5194/acp-11-5959-2011, 2011.

Ma, N., Zhao, C. S., Muller, T., Cheng, Y. F., Liu, P. F., Deng, Z. Z., Xu, W. Y., Ran, L., Nekat, B., van Pinxteren, D., Gnauk, T., Mueller, K., Herrmann, H., Yan, P., Zhou, X. J., and Wiedensohler, A.: A new method to determine the mixing state of light absorbing carbonaceous using the measured aerosol optical properties and number size distributions, Atmospheric Chemistry and Physics, 12, 2381-2397, 10.5194/acp-12-2381-2012, 2012.

Mackowski, D. W., and Mishchenko, M. I.: Calculation of the T matrix and the scattering matrix for ensembles of spheres, J. Opt.

Soc. Am. A-Opt. Image Sci. Vis., 13, 2266-2278, 10.1364/josaa.13.002266, 1996.

Mackowski, D. W.: A general superposition solution for electromagnetic scattering by multiple spherical domains of optically active media, Journal of Quantitative Spectroscopy & Radiative Transfer, 133, 264-270, 10.1016/j.jqsrt.2013.08.012, 2014.

Majdi, M., Kim, Y., Turquety, S., and Sartelet, K.: Impact of mixing state on aerosol optical properties during severe wildfires over the Euro-Mediterranean region, Atmospheric Environment, 220, 11, 10.1016/j.atmosenv.2019.117042, 2020.

Martins, J. V., Artaxo, P., Liousse, C., Reid, J. S., Hobbs, P. V., and Kaufman, Y. J.: Effects of black carbon content, particle size, and mixing on light absorption by aerosols from biomass burning in Brazil, J. Geophys. Res.-Atmos., 103, 32041-32050, 10.1029/98jd02593, 1998.

Moffet, R. C., O'Brien, R. E., Alpert, P. A., Kelly, S. T., Pham, D. Q., Gilles, M. K., Knopf, D. A., and Laskin, A.: Morphology and mixing of black carbon particles collected in central California during the CARES field study, Atmospheric Chemistry and Physics, 16, 14515-14525, 10.5194/acp-16-14515-2016, 2016.

Moosmuller, H., Chakrabarty, R. K., and Arnott, W. P.: Aerosol light absorption and its measurement: A review, Journal of Quantitative Spectroscopy & Radiative Transfer, 110, 844-878, 10.1016/j.jqsrt.2009.02.035, 2009.

Nakayama, T., Ikeda, Y., Sawada, Y., Setoguchi, Y., Ogawa, S., Kawana, K., Mochida, M., Ikemori, F., Matsumoto, K., and Matsumi, Y.: Properties of light-absorbing aerosols in the Nagoya urban area, Japan, in August 2011 and January 2012: Contributions of brown carbon and lensing effect, J. Geophys. Res.-Atmos., 119, 12721-12739, 10.1002/2014jd021744, 2014.

Ning, Z., Chan, K. L., Wong, K. C., Westerdahl, D., Mocnik, G., Zhou, J. H., and Cheung, C. S.: Black carbon mass size distributions of diesel exhaust and urban aerosols measured using differential mobility analyzer in tandem with Aethalometer, Atmospheric Environment, 80, 31-40, 10.1016/j.atmosenv.2013.07.037, 2013.

Onasch, T. B., Trimborn, A., Fortner, E. C., Jayne, J. T., Kok, G. L., Williams, L. R., Davidovits, P., and Worsnop, D. R.: Soot Particle Aerosol Mass Spectrometer: Development, Validation, and Initial Application, Aerosol Science and Technology, 46, 804-817, 10.1080/02786826.2012.663948, 2012.

Peng, J. F., Hu, M., Guo, S., Du, Z. F., Zheng, J., Shang, D. J., Zamora, M. L., Zeng, L. M., Shao, M., Wu, Y. S., Zheng, J., Wang, Y., Glen, C. R., Collins, D. R., Molina, M. J., and Zhang, R. Y.: Markedly enhanced absorption and direct radiative forcing of black carbon under polluted urban environments, Proceedings of the National Academy of Sciences of the United States of America, 113, 4266-4271, 10.1073/pnas.1602310113, 2016.

Petzold, A., and Schonlinner, M.: Multi-angle absorption photometry - a new method for the measurement of aerosol light absorption and atmospheric black carbon, Journal of Aerosol Science, 35, 421-441, 10.1016/j.jaerosci.2003.09.005, 2004.

Petzold, A., Ogren, J. A., Fiebig, M., Laj, P., Li, S. M., Baltensperger, U., Holzer-Popp, T., Kinne, S., Pappalardo, G., Sugimoto, N., Wehrli, C., Wiedensohler, A., and Zhang, X. Y.: Recommendations for reporting "black carbon" measurements, Atmospheric Chemistry and Physics, 13, 8365-8379, 10.5194/acp-13-8365-2013, 2013.

Ram, K., and Sarin, M. M.: Absorption Coefficient and Site-Specific Mass Absorption Efficiency of Elemental Carbon in Aerosols over Urban, Rural, and High-Altitude Sites in India, Environmental Science & Technology, 43, 8233-8239, 10.1021/es9011542,

2009.

Ramachandran, S., and Rajesh, T. A.: Black carbon aerosol mass concentrations over Ahmedabad, an urban location in western India: Comparison with urban sites in Asia, Europe, Canada, and the United States, J. Geophys. Res.-Atmos., 112, 19, 10.1029/2006jd007488, 2007.

Ramanathan, V., and Carmichael, G.: Global and regional climate changes due to black carbon, Nature Geoscience, 1, 221-227, 10.1038/ngeo156, 2008.

Ran, L., Deng, Z. Z., Wang, P. C., and Xia, X. A.: Black carbon and wavelength-dependent aerosol absorption in the North China Plain based on two-year aethalometer measurements, Atmospheric Environment, 142, 132-144, 10.1016/j.atmosenv.2016.07.014, 2016a.

Ran, L., Deng, Z. Z., Xu, X. B., Yan, P., Lin, W. L., Wang, Y., Tian, P., Wang, P. C., Pan, W. L., and Lu, D. R.: Vertical profiles of black carbon measured by a micro-aethalometer in summer in the North China Plain, Atmospheric Chemistry and Physics, 16, 10441-10454, 10.5194/acp-16-10441-2016, 2016b.

Sandradewi, J., Prevot, A. S. H., Szidat, S., Perron, N., Alfarra, M. R., Lanz, V. A., Weingartner, E., and Baltensperger, U.: Using aerosol light absorption measurements for the quantitative determination of wood burning and traffic emission contributions to particulate matter, Environmental Science & Technology, 42, 3316-3323, 10.1021/es702253m, 2008.

Schmid, O., Artaxo, P., Arnott, W. P., Chand, D., Gatti, L. V., Frank, G. P., Hoffer, A., Schnaiter, M., and Andreae, M. O.: Spectral light absorption by ambient aerosols influenced by biomass burning in the Amazon Basin. I: Comparison and field calibration of absorption measurement techniques, Atmospheric Chemistry and Physics, 6, 3443-3462, 10.5194/acp-6-3443-2006, 2006.

Schwarz, J. P., Gao, R. S., Fahey, D. W., Thomson, D. S., Watts, L. A., Wilson, J. C., Reeves, J. M., Darbeheshti, M., Baumgardner, D. G., Kok, G. L., Chung, S. H., Schulz, M., Hendricks, J., Lauer, A., Karcher, B., Slowik, J. G., Rosenlof, K. H., Thompson, T. L., Langford, A. O., Loewenstein, M., and Aikin, K. C.: Single-particle measurements of midlatitude black carbon and light-scattering aerosols from the boundary layer to the lower stratosphere, J. Geophys. Res.-Atmos., 111, 15, 10.1029/2006jd007076, 2006.

Schwarz, J. P., Spackman, J. R., Fahey, D. W., Gao, R. S., Lohmann, U., Stier, P., Watts, L. A., Thomson, D. S., Lack, D. A., Pfister, L., Mahoney, M. J., Baumgardner, D., Wilson, J. C., and Reeves, J. M.: Coatings and their enhancement of black carbon light absorption in the tropical atmosphere, J. Geophys. Res.-Atmos., 113, 10, 10.1029/2007jd009042, 2008.

Sharma, S., Brook, J. R., Cachier, H., Chow, J., Gaudenzi, A., and Lu, G.: Light absorption and thermal measurements of black carbon in different regions of Canada, J. Geophys. Res.-Atmos., 107, 11, 10.1029/2002jd002496, 2002.

Shiraiwa, M., Kondo, Y., Moteki, N., Takegawa, N., Miyazaki, Y., and Blake, D. R.: Evolution of mixing state of black carbon in polluted air from Tokyo, Geophys. Res. Lett., 34, 5, 10.1029/2007gl029819, 2007.

Shiraiwa, M., Kondo, Y., Iwamoto, T., and Kita, K.: Amplification of Light Absorption of Black Carbon by Organic Coating, Aerosol Science and Technology, 44, 46-54, 10.1080/02786820903357686, 2010.

Sorensen, C. M.: Light scattering by fractal aggregates: A review, Aerosol Science and Technology, 35, 648-687, 10.1080/027868201316900007, 2001.

Truex, T. J., and Anderson, J. E.: Mass monitoring of carbonaceous aerosols with a spectrophone, Atmospheric Environment, 13, 507-509, 10.1016/0004-6981(79)90143-4, 1979.

Wu, C., Ng, W. M., Huang, J. X., Wu, D., and Yu, J. Z.: Determination of Elemental and Organic Carbon in PM2.5 in the Pearl River Delta Region: Inter-Instrument (Sunset vs. DRI Model 2001 Thermal/Optical Carbon Analyzer) and Inter-Protocol Comparisons (IMPROVE vs. ACE-Asia Protocol), Aerosol Science and Technology, 46, 610-621, 10.1080/02786826.2011.649313, 2012.

Zhang, R. Y., Khalizov, A. F., Pagels, J., Zhang, D., Xue, H. X., and McMurry, P. H.: Variability in morphology, hygroscopicity, and optical properties of soot aerosols during atmospheric processing, Proceedings of the National Academy of Sciences of the United States of America, 105, 10291-10296, 10.1073/pnas.0804860105, 2008.

Zhang, Y. X., Zhang, Q., Cheng, Y. F., Su, H., Li, H. Y., Li, M., Zhang, X., Ding, A. J., and He, K. B.: Amplification of light absorption of black carbon associated with air pollution, Atmospheric Chemistry and Physics, 18, 9879-9896, 10.5194/acp-18-9879-2018, 2018.

Zhao, G., Tan, T. Y., Zhao, W. L., Guo, S., Tian, P., and Zhao, C. S.: A new parameterization scheme for the real part of the ambient urban aerosol refractive index, Atmospheric Chemistry and Physics, 19, 12875-12885, 10.5194/acp-19-12875-2019, 2019a.

Zhao, G., Tao, J. C., Kuang, Y., Shen, C. Y., Yu, Y. L., and Zhao, C. S.: Role of black carbon mass size distribution in the direct aerosol radiative forcing, Atmospheric Chemistry and Physics, 19, 13175-13188, 10.5194/acp-19-13175-2019, 2019b.

Zhao, G., Yu, Y., Tian, P., Li, J., Guo, S., and Zhao, C.: Evaluation and Correction of the Ambient Particle Spectral Light Absorption Measured Using a Filter-based Aethalometer, Aerosol and Air Quality Research, 20, 1833-1841, 10.4209/aaqr.2019.10.0500, 2020.

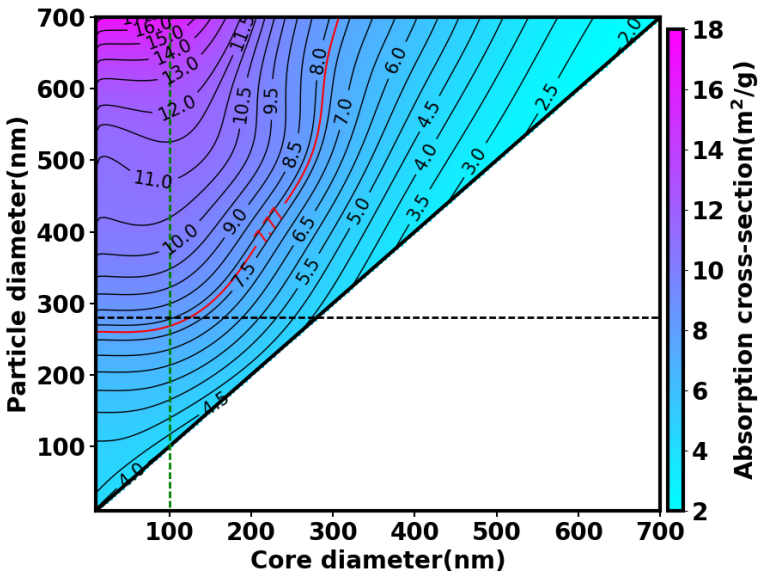

Figure 1. Variations in MAC as a function of D_{BC} and $D_{particle}$, calculated by the concentric core-shell Mie model at the wavelength of 880 nm. The red solid line is the constant MAC value used in AE33. The bold black solid line is the 1:1 line that presents the variations in MAC for pure BC particles with different D_{BC}. The horizontal black dashed line distinguishes particles with a diameter of 280 nm while the vertical green dashed line indicates a D_{BC} of 100 nm.

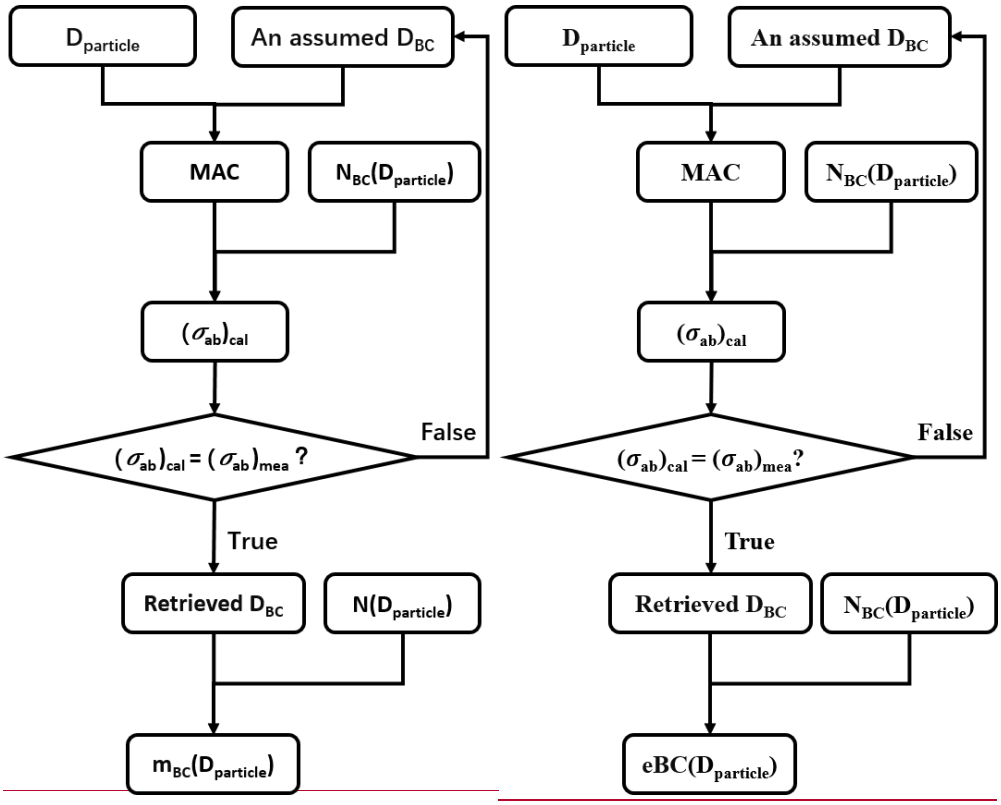

Figure 2. Schematic diagram of the iterative algorithm for retrieving the ~~m_{BC}~~ EBC at a fixed particle diameter based on the look-up table of MAC, particle size and core size. $(\sigma_{ab})_{cal}$ and $(\sigma_{ab})_{mea}$ represent calculated and measured absorption coefficients, respectively. $N_{BC}(D_{particle})$ indicates the number concentration of particle containing BC at the given $D_{particle}$.

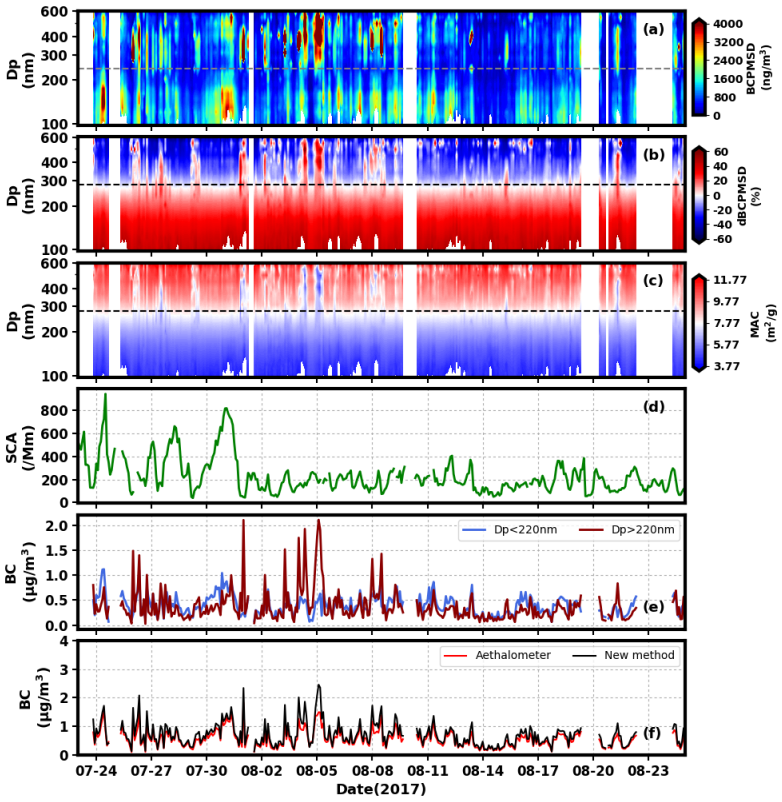

Figure 3. Time series of (a) the BCPMSD derived from the new~~ly proposed~~ method proposed in this work. ~~(~~The dashed line indicates the particle size of 240 nm~~)~~; (b) relative deviations between BCPMSD derived from the new method (varied MAC) and ~~a~~ constant MAC ~~of~~ at 7.77 m^2/g ~~(~~. The dashed line indicates the particle size of 280 nm~~)~~; (c) the size-resolved MAC ~~determined during the process of retrieving BCPMSD (~~. The dashed line indicates the particle size of 280 nm~~)~~; (d) the scattering coefficients ~~simultaneously measured with the size-resolved ~~$_{ab}$~~~~at 525 nm; (e) the ~~m_{BC}~~ EBC integrated for particles smaller than ~~280~~ 220 nm (blue) and larger than ~~280~~ 220 nm (red); and (f) the ~~m_{BC}~~ EBC determined by the new method (black) and ~~the~~ constant MAC of 7.77 m^2/g (red).

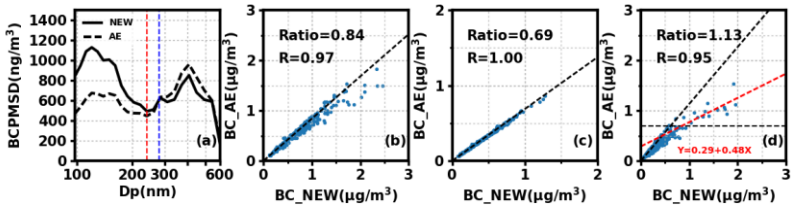

Figure 4. Comparison between the EBC derived from the new~~ly proposed~~ method and ~~using from~~ constant MAC of 7.77 m^2/g used by AE33 ~~in the derived results of~~. (a) shows the results of the BCPMSD, ~~(~~the dashed black line ~~shows~~ is the result~~s~~

of ~~AE33~~ constant MAC of 7.77 m^2/g used by AE33, ~~while~~ and the solid black line represents the results from the new method; the dashed red line ~~represents~~ is the split line ~~(diameter~~ of 240 nm~~)~~ between ~~finer~~fine mode and ~~coarser~~coarse mode ~~for BCPMSD;~~ , and the dashed blue line ~~indicates~~ is the split line ~~(~~of 280 nm ~~of diameter)~~ between the opposite tendencies of deviations in ~~the m_{BC}~~ BCPMSD~~calculated from the new method and the aethalometer)~~; (b) the bulk ~~m_{BC}~~ EBC ~~for particles ranging~~integrated from 97 nm to 602 nm; (c) the fine mode ~~m_{BC}~~ EBC ~~for the finer mode (~~integrated from 97 nm ~~—~~to 280 nm~~)~~; (d) the ~~m_{BC}~~ coarse mode EBC ~~for the coarser mode (~~integrated from 280 ~~—~~to 606 nm~~)~~; the dashed black line represents boundary of 0.7 $\mu g/m^3$ and the red dashed line is the regression line ~~of~~ for the ~~m_{BC}~~ EBC ~~derived from AE and the new method when m_{BC} is~~ larger than 0.7 $\mu g/m^3$.

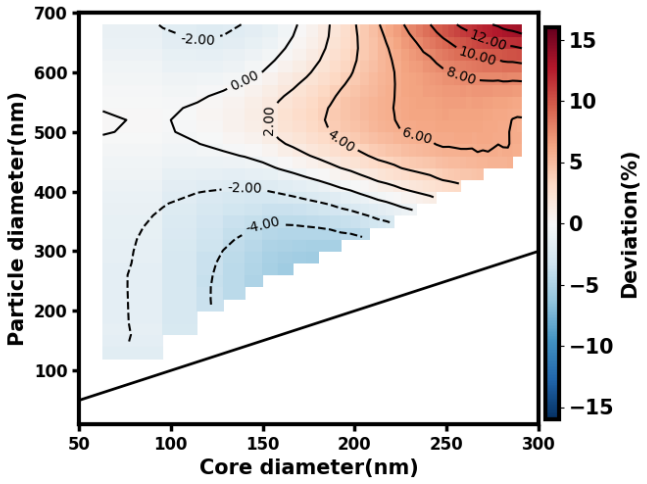

Figure 5. Relative deviations of MAC values calculated by idealized concentric core-shell model and letting BC particles be in the form of cluster-like aggregates. The solid line is 1:1 line.

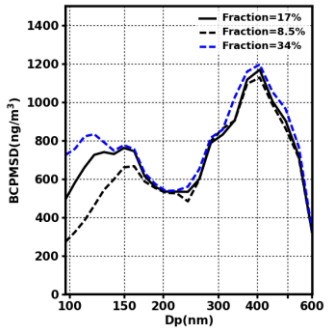

Figure 6. The derived BCPMSD by using different constant BC-containing particle fraction. The solid black line represents

带格式的: 字体: (默认) Times New Roman, 加粗

带格式的: 定义网格后自动调整右缩进, 调整中文与西文文字的间距, 调整中文与数字的间距

带格式的: 字体: 10 磅

the result derived from a fraction of 17%. The dashed black line and blue line show the results derived from a fraction of half of 8.5% and double of 34%.

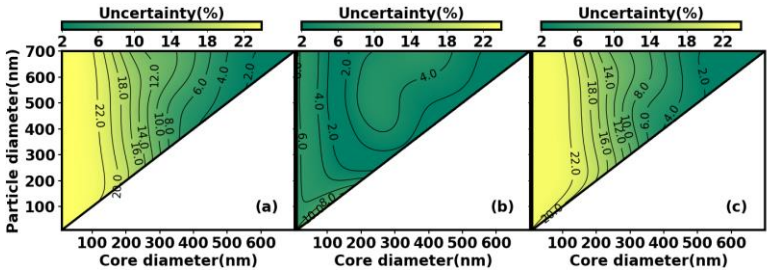

Figure ~~5~~7. Uncertainty in MAC of BC when (a) real part of RI ranges from 1.5 to 2.0 and imaginary part ranges from 0.5 to 1.1; (b) real part of RI ranges from 1.5 to 2.0 and imaginary part is fixed at 0.8 and (c) real part of RI is fixed at 1.75 and imaginary part ranges from 0.5 to 1.1. The bold black solid line is the 1:1 line and presents the uncertainty of MAC for pure BC particles with different RI.

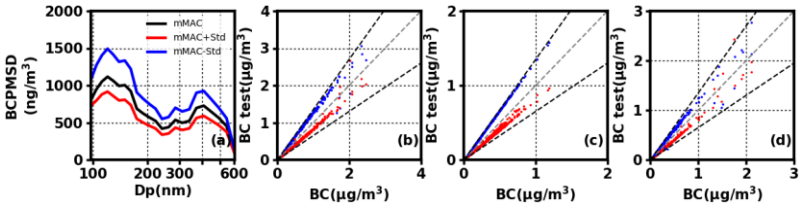

Figure ~~6~~8. (a) The BCPMSD calculated by using the look up table with mean MAC (black line), mean MAC plus the corresponding standard deviation (red line) and mean MAC minus the corresponding standard deviation (blue line); the ~~mBC~~ EBC derived by the look up table with mean MAC versus those derived by the look up table with mean MAC plus standard deviation (red dots) or mean MAC minus standard deviation (blue dots) for (b) aerosol particles ranging from 97–602 nm; (c) aerosol particles ranging from 97–240 nm (~~finer~~fine mode); and (d) aerosol particles ranging from 240–602 nm (~~coarser~~coarse mode). The dashed black line represents the 35% deviation from the 1:1 line (dashed grey lines).